UNIVERSIDADE D
COIMBRA

João Paulo Ferreira da Silva

Preformulation Studies on Roxadustat

Dissertação no âmbito do Mestrado em Tecnologias do Medicamento orientado pelo Professor Doutor João Carlos Canotilho Lage e pela Professora Doutora Maria Ermelinda da Silva Eusébio e apresentada à Faculdade de Farmácia da Universidade de Coimbra

Setembro de 2023

João Paulo Ferreira da Silva

PREFORMULATION STUDIES ON ROXADUSTAT

Dissertação no âmbito do Mestrado em Tecnologias do Medicamento orientado pelo Professor Doutor João Carlos Canotilho Lage e pela Professora Doutora Maria Ermelinda da Silva Eusébio e apresentada à Faculdade de Farmácia da Universidade de Coimbra

Setembro de 2023

Para os meus avós, mãe, pai e irmã

AGRADECIMENTOS

E chega ao final este tão longo percurso. Foram 5 anos nesta montanha-russa que é Coimbra, cheia de altos e baixos, cheia de amizades, aventuras, trabalho e muitas memórias que levo para a vida. Desde a "capa negra", os amigos, a casa e as pessoas nela onde vivi a maior parte do meu tempo nesta bela cidade, a universidade onde estudei durante 4 anos até à beleza única que é Coimbra, só tenho a agradecer por tudo o que experienciei nestes anos todos.

Aos meus orientadores, o Professor Doutor João Canotilho e a Professora Doutora Ermelinda Eusébio, o meu enorme obrigado por toda a ajuda, disponibilidade, paciência e carinho que sempre tiveram comigo ao longo deste ano. Nunca esquecerei todo o apoio e confiança que depositaram em mim.

Ao Professor Doutor Ricardo Castro, um grande obrigado por toda a disponibilidade que sempre mostrou para comigo e por me ter ajudado a desenvolver este projeto.

Ao Mestre João Batista, por toda a paciência que teve comigo ao longo deste ano. Desculpa "moer-te a cabeça", irei ficar sempre grato por toda a tua ajuda.

Ao Guilherme, Amanda, Inês e Joana, um obrigado por todos os bons momentos e ajuda que me proporcionaram.

A todo o grupo de Termodinâmica e Química do Estado Sólido e ao UCQFarma, por me aceitarem e acolherem.

Ao Duarte da Silva, não há palavras para descrever o quão agradecido estou pela melhor amizade que alguém poderia ter ao longo destes 5 anos. Obrigado por todos os momentos que passei contigo, obrigado pelas gargalhadas, pelo apoio, pelos concelhos, por todo o percurso académico partilhado. Que estes 5 anos sejam só o início duma longa amizade.

Aos meus amigos da licenciatura, em especial ao Miguel, aos meus padrinhos e afilhada de praxe, sem vocês nada teria sido o mesmo. Obrigado por fazerem Coimbra inesquecível.

Aos meus amigos da terrinha, obrigado por sempre estarem presente nos momentos de mais aflição e por todo o apoio e confiança que me deram sempre. Aos bons momentos que vivemos e aos que viveremos.

À minha família, por todo o carinho e apoio que sempre me deram, o meu grande obrigado.

Aos meus avós, um especial obrigado por todo o apoio que me deram no meu percurso académico. Obrigado por me fazerem sentir sempre um neto amado, do qual têm muito orgulho. Nunca na vida irei conseguir agradecer o que fizeram por mim.

Por último, às pessoas mais importantes da minha vida, à minha mãe, ao meu pai e à minha irmã, obrigado por todo o amor incondicional que sempre me deram, obrigado por me terem proporcionado estes 5 anos tão importantes da minha vida, obrigado por todo o apoio e por todo o carinho. Foram e irão ser para sempre os meus pilares motivacionais e emocionais. Sem vocês nada disto teria sido possível e, portanto, irei continuar a minha vida a agradecer-vos e a deixar-vos orgulhosos.

INDEX

LIST OF FIGURES

LIST OF TABLES

ABBREVIATIONS

ACA – Ascorbic Acid

ADME – Absorption, Distribution, Metabolism, Excretion

API – Active Pharmaceutical Ingredient

BCS – Biopharmaceutical Classification System

BENZ – Benzamide

BPA – 1,2-Bis(4-pyridyl) ethane

BPY – 4,4 -Bipyridyl

BZA – Benzoic Acid

CAF – Caffeine

CIA – Citric Acid

CKD – Chronic Kidney Disease

CYS – Cysteine

DSC – Differential Scanning Calorimetry

EtOH - Ethanol

FA – Folic Acid

FDA – Food and Drug Administration

FTIR-ATR – Fourier transform infrared spectroscopy with Attenuated Total Reflectance module

GFR – Glomerular Filtration Rate

GRAS – Generally Recognized As Safe

HIF – Hypoxia-Inducible Factor

HIF-PH – Hypoxia-Inducible Factor Prolyl Hydroxylase

HIS – L-Histidine

ISO – Isonicotinamide

LAG – Liquid Assisted Grinding

MeOH – Methanol

NG – Neat Grinding

NICO – Nicotinamide

PD – Pharmacodynamics

PK – Pharmacokinetics

PYX – Pyridoxine

PYZ – Pirazine

PZA – Pyrazinamide

ROXA – Roxadustat

SCXRD – Single Crystal X-ray Diffraction

TGA – Thermogravimetric Analysis

THEO – Theophylline

TRP – Tryptophan

XRPD – X-ray Powder Diffraction

ABSTRACT

From an early stage, in the research and development of a new active pharmaceutical ingredient, it is crucial to perform preformulation studies. These studies enable the physicochemical characterization of active pharmaceutical ingredients to ensure their stability, safety, and efficacy, achieving adequate and desirable bioavailability, which helps prevent manufacturing problems, optimize drug performance, and create room for innovation.

This work aims at investigating the solid state behavior of roxadustat and the screening and characterization of roxadustat containing multicomponent solid forms. The solubility of promising solid forms, from a pharmaceutical point of view, was also evaluated in aqueous HCl simulating the pH of the medium where this active substance is absorbed (stomach: pH≈3).

Roxadustat is a small molecule, administered orally, which inhibits prolyl hydroxylase by increasing the transcription activity of the hypoxia-inducible factor (HIF), stabilizing the HIF-α subunits. The increase in transcriptional activity promotes erythropoiesis. It is approved for the clinical treatment of chronic kidney disease- associated anemia in China, the European Union, Japan, South Korea, and Chile.

It is important to know how the pharmaceutical active ingredient behaves in the solid state and carefully choose the ideal solid form for pharmaceutical development.

In this work, as characterization methods, calorimetric (differential scanning calorimetry,) and spectroscopic (ultraviolet and Fourier transform infrared spectroscopies, powder X-ray diffraction) methods were used. Mechanochemistry (neat and liquid assisted grinding, LAG) was used as screening methodology.

Different molar ratios were tested for binary mixtures of roxadustat and coformers These were selected according to the possibility of establishing heterosynthons with roxadustat and also considering their pharmaceutical interest - pyrazine, 1,2-bis(4-pyridyl)ethane, 4,4 bipyridyl, benzamide, nicotinamide, isonicotinamide, pyrazinamide, caffeine, theophylline, L-histidine, cysteine, tryptophan, pyridoxine, folic acid, citric acid, benzoic acid, and ascorbic acid.

Liquid assisted grinding resulted in the synthesis of new cocrystals with hydrogen bond acceptor coformers such as 1,2-bis(4-pyridyl)ethane, 4,4'-bipyridil, pyrazine as well as with caffeine. No association occurred with theophylline; the other xanthine investigated.

Cocrystals were also obtained by LAG with benzamide and nicotinamide, but not with pyrazinamide, which is more complex concerning functional groups.

Two coamorphous phases, roxadustat:folic acid (1:1) and roxadustat:pyridoxine (1:1), were synthesized by neat grinding, which is quite promising for pharmaceutical development.

In summary, this investigation has provided useful information on the behavior of roxadustat in the solid state, with new cocrystals and amorphous phases identified, and interesting results were obtained regarding the solubility of this drug, when using the coamorphous mixture with pyridoxine.

Keywords: roxadustat; preformulation studies; cocrystals; coamorphous; solubility.

RESUMO

Na pesquisa e desenvolvimento de uma nova substância ativa é crucial a realização de estudos de pré-formulação. Estes estudos permitem a caracterização físico-química das substâncias ativas por forma a garantir a sua estabilidade, segurança e eficácia, contribuindo para uma biodisponibilidade adequada e desejável, o que ajuda a prevenir problemas de produção, otimizar o desempenho do medicamento criando espaço para a inovação.

Este trabalho tem como objetivo investigar o comportamento do estado sólido de roxadustate e efetuar o *screening* e a caracterização de formas sólidas multicomponente deste ativo farmacêutico. Foi também avaliada a solubilidade das formas sólidas promissoras do ponto de vista farmacêutico, em HCl aquoso para simular o pH do meio onde esta substância ativa é absorvida (estômago: pH≈1-3).

O roxadustate é uma pequena molécula, administrada por via oral, inibidora da prolil hidroxilase incrementando a atividade de transcrição do fator indutor de hipoxia (HIF), estabilizando as subunidades HIF-α. O incremento da atividade transcricional promove a eritropoiese. Está aprovado para o tratamento clínico da anemia associada à doença renal crónica na China, na União Europeia, no Japão, na Coreia do Sul e no Chile.

É importante conhecer o comportamento desta substância ativa no estado sólido e escolher cuidadosamente a forma sólida ideal para o desenvolvimento farmacêutico. Neste trabalho, como métodos de caracterização, foram utilizados métodos calorimétricos (calorimetria diferencial de varrimento) e espectroscópicos (espectroscopia no ultravioleta, espectroscopia de infravermelho por transformada de Fourier e difração de raios-X de pó). A mecanoquímica (moagem sem solvente, NG e assistida por solvente, LAG) foi utilizada como metodologia de síntese.

Foram testadas misturas binárias de diferentes proporções molares de roxadustate e coformadores. Estes foram selecionados de acordo com a probabilidade de estabelecimento de heterossintões com o roxadustate e tendo em conta também o interesse farmacêutico. Assim são: pirazina, 1,2-bis(4-piridil) etano, 4,4'-bipiridil, benzamida, nicotinamida, isonicotinamida, pirazinamida, cafeína, teofilina, L-histidina, cisteína, triptofano, piridoxina, ácido fólico, ácido cítrico, ácido benzoico e ácido ascórbico.

A moagem assistida por solvente resultou na síntese de novos cocristais com os referidos coformadores aceitadores de ligações de hidrogénio, como o 1,2-bis(4-piridil) etano, o 4,4'-bipiridil, a pirazina e a cafeína. Não foi observada interação com a teofilina, a outra xantina investigada.

Também foram sintetizados cocristais por LAG tendo como coformador a benzamida e a nicotinamida, mas não com a pirazinamida, que é mais complexa no que diz respeito a grupos funcionais.

Duas fases coamorfas, roxadustate:ácido fólico (1:1) e roxadustate:piridoxina (1:1), foram sintetizadas por moagem sem adição de solvente, o que é bastante promissor para o desenvolvimento farmacêutico.

Em resumo, esta investigação forneceu informações úteis sobre o comportamento do roxadustate no estado sólido, com a obtenção de novos cocristais e fases amorfas identificadas, bem como resultados interessantes relativamente à solubilidade do API quando usada a mistura coamorfa com piridoxina.

Palavras-chave: roxadustate; estudos de pré-formulação; cocristais; coamorfos; solubilidade.

1. INTRODUCTION

1.1. Polymorphism

Determining exactly which solid form of an active pharmaceutical ingredient (API) should be chosen for formulation, clinical trials and scale up is a crucial step in the drug development process.[1]

Solid materials can exist in two or more crystalline forms. This phenomenon is known as polymorphism, where chemical substances have different arrangements or conformations of the constituents in the crystal lattice. The polymorphic forms differ in their physicochemical properties despite sharing a similar chemical structure because they usually have different intermolecular interactions including van der Waals and hydrogen bonds. These different intermolecular interactions affect their chemical and physical properties, such as dissolution, stability, solubility, melting point, hygroscopicity, and they also influence important drug outcomes like drug efficacy, bioavailability, and toxicity.[2]

This phenomenon is widely studied in active pharmaceutical ingredients, so its complete characterization is very important, including thermodynamic and kinetic stability.

Several analytical methods have been used to characterize the crystalline form of a drug throughout its development process. The techniques used include X-ray powder diffraction (XRPD), single crystal X-ray diffraction (SCXRD), thermal methods such as differential scanning calorimetry (DSC), thermogravimetric analysis (TGA), and microscopic and spectroscopic methods (fourier transform infrared spectroscopy with ATR module and Raman spectroscopy, for instance).

Usually, there are two types of polymorphism. On one hand, there are monotropic systems, where only one polymorphic is stable over the entire temperature range below the melting point of the solid material, at a specified pressure. On the other hand, there are enantiotropic systems, where one of the polymorphs represents the form that is most stable over a given temperature and pressure range, while the other is more stable over a different temperature and pressure range.[3,4]

It is important to know the most stable polymorph to carefully choose the ideal solid form for development.

1.2. API Solid Forms

A compound in the solid state is generally chemically more stable than in solution where its degradation may be more extensive and faster.[5] Solid formulations are also easier to prepare and are less likely to contain impurities.[6]

As already mentioned, APIs can have different crystalline forms. This phenomenon is termed as polymorphism. Crystalline forms of APIs may have low aqueous solubility, and it is sometimes necessary to use their amorphous phase, i.e., without organized crystalline arrangement, or a multicomponent form in case it is more stable.[7]

Figure 1 shows a schematic representation of different crystalline solid forms of active pharmaceutical ingredients.[8]

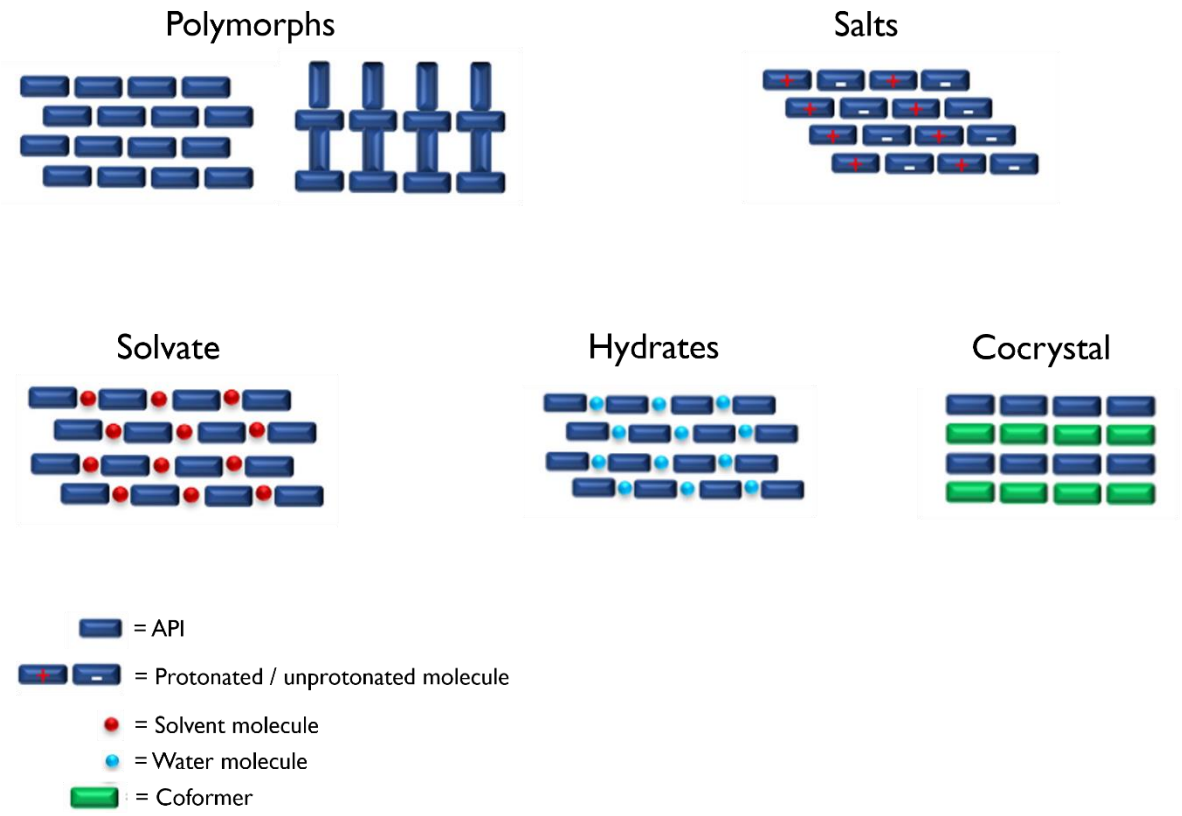

Figure 1 - Schematic representation of different crystalline solid forms of active pharmaceutical ingredients

1.2.1. Cocrystals

Cocrystals are multicomponent systems, consisting of two or more neutral molecular species, API(s) and coformer(s), both solids at room temperature, which interact by specific non-covalent bonds in a stoichiometric relation. It is important to note that cocrystals can be formed with a given coformer at different stoichiometric ratios.[9]

These solid forms have a significant impact in the development of pharmaceutical drugs by providing possibilities to control the structure and composition and, therefore, to improve physicochemical and mechanical properties of drugs, such as, stability, solubility, dissolution profile, permeability, hygroscopicity and bioavailability.[9–13]

In order to synthesize cocrystals, it is important to carefully choose the coformers. The choice of coformers should be made considering the functional groups capable of forming supramolecular hetero or homosynthons with the API(s).[14] These substances frequently exhibit the capacity to generate hydrogen bonds and are water soluble.

On the safety profile of coformers, they must be in accordance with GRAS (generally recognized as safe substances) in order to be accepted in the market. Substances with high solubility, such as nicotinamide, isoniazid, caffeine, pyrazinamide and isonicotinamide, are normally used as coformers.[14,15]

When APIs are used as coformers, the final product is called drug-drug cocrystal. A new approach in drug development is the use of this type of cocrystals. They enable the combination of substances formerly used in combinatory therapy in a single solid form, improving their synergistic effects and individual physicochemical properties. [16]

Pharmaceutical cocrystal design and production is a popular preformulation study method. There are different methods for preparing cocrystals, which can be generally classified as solid-state or solution-based methods. The first one use very little or no solvent, while solution-based methods involve a large excess of solvent.[17] In the present work, to study the formation of cocrystals, it was used a solvent-free method, mechanochemistry, more precisely, neat grinding (NG) and liquid assisted grinding (LAG). Since no solvent is used in neat grinding, which can help the cocrystallization procedure, it is not always possible to obtain the cocrystals in a reproducible way. LAG has been successfully used for cocrystallization in different cases where solid-state milling has failed and is considered superior to other conventional methods, such as slow evaporation or slurry-based methods.[17,18]

1.2.2. Solvates

Solvates represent a fascinating aspect of solid-state chemistry, where the interaction between a solute and a solvent goes beyond a mere dissolution process and leads to the formation of distinct crystalline structures.

Similar to cocrystals, solvates are multicomponent solid forms, associating an API and a substance which is a liquid when pure at ambient conditions. This type of solid form is also stabilized by hydrogen bonds and van der Walls intermolecular interactions.[19,20]

Solvates exhibit distinctive characteristics compared to anhydrous or non-solvated counterparts. These properties arise from the presence of solvent molecules, which can affect crystal packing, lattice energy, thermal stability, and even the colour of the crystal. Moreover, solvates often display altered solubility profiles, dissolution rates, and mechanical properties, making them of considerable interest in pharmaceuticals, materials science, and separation technologies.[21]

When the solvent in the crystal lattice is water, a special type of solvent is present, a hydrate. The number of intermolecular interactions (internal energy and enthalpy) and the degree of crystalline disorder (entropy) are both influenced by the presence of water molecules. Solubility, dissolution rate, solid state stability, free energy, thermodynamic parameters, and bioavailability of hydrated APIs are all affected. [19,22]

1.2.3. Amorphous

Besides the solid forms shown if Figure 1, amorphous phases must also be considered. Amorphous solids are characterized by having a disordered structure compared to the crystalline form and have a higher Gibbs free energy. This lack of order in the molecules of an amorphous solid leads to a higher apparent water solubility, dissolution rate, and oral absorption, which consequently improves bioavailability.[23,24]

Amorphous compounds have garnered substantial attention in the pharmaceutical industry due to their increased solubility and bioavailability compared to their crystalline counterparts. However, their inherent chemical and physical instability means that these solid forms are not so often used for formulation development. This instability of amorphous compounds occurs due to the tendency of these solid forms to recrystallize, that is, to return to their most stable energy state, which is the crystalline state.[25–27]

Amorphous materials may be prepared, for instance, by grinding or by supercooling a molten phase. This method involves the rapid cooling of molten substances, while the molecules

reorganize so slowly that they are unable to obtain a representative sample of the configurations within the time frame permitted by the cooling rate. [28]

Amorphous solids have provided an attractive alternative for solubility problems, however, understanding and overcoming their chemical and physical instability has not yet been fully clarified.

1.2.4. Coamorphous

Coamorphous compounds, an emerging class of materials, offer a novel approach to overcoming limitations associated with traditional amorphous and crystalline forms.[29]

Solid forms known as coamorphous systems are developed by the combination of an API and a coformer, such as cocrystals. In this particular type of systems, the API is amorphized with a coformer to create a single amorphous phase at a specific stoichiometric ratio resulting in a coamorphous system.[30]

The pharmaceutical industry has embraced coamorphous solids as a means to address challenges associated with poor solubility and stability of certain drugs. By coforming an active pharmaceutical ingredient (API) with a suitable coformer, researchers can create a coamorphous system that enhances solubility, leading to faster dissolution and potentially better therapeutic outcomes. Additionally, coamorphous systems can mitigate issues related to polymorphism and recrystallization, offering improved stability for sensitive APIs.[31,32]

Although these solid forms present themselves as a good alternative to drugs that are poorly soluble in water, their chemical and physical instability, like that of amorphous forms, is still a barrier to be overcome.[33–35]

1.3. Biopharmaceutical Classification System (BCS)

The Biopharmaceutical Classification System (BCS) is a scientific method of classifying drugs according to their aqueous solubility and intestinal permeability, which makes it a very effective indicator of bioavailability. In BCS drugs are divided into four classes, in which drugs with higher solubility and permeability constitute class I and those with lower solubility and permeability belongs to class IV, as shown in Figure 2.[36,37]

Currently, most new chemical entities are classified as class II or class IV, meaning that most new drug candidate compounds would have poor aqueous solubility.[38] This is a difficult problem to overcome, since these types of drugs require higher doses to have a therapeutic effect, which means that there will be a greater risk of toxicity.[38,39]

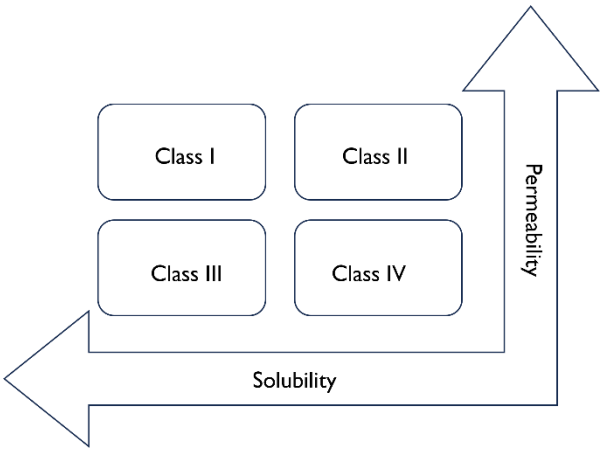

Figure 2 - The Biopharmaceutical Classification System

1.4. Solubility

Solubility is a physical constant and refers to the maximum amount of a substance that can dissolve in a given amount of solvent at a given temperature and pressure. It is an important concept in the pharmaceutical domain since it can control the bioavailability of a drug substance. This parameter is also important with regard to the characterization of a substance since it provides information about its molecular structure and possible intermolecular interactions.[40]

Solubility is influenced by several factors, including temperature, pressure, and the chemical nature of both the solute and solvent. Substances with similar polarities tend to dissolve in one another, while polar and nonpolar substances usually do not mix well.[41,42]

The Gibbs free energy change (ΔG) determines whether a solute will dissolve in a solvent. If ΔG is negative, the process is spontaneous, indicating favourable solubility. Conversely, a positive ΔG suggests limited solubility.[41]

To assess the solubility of a substance, it is important to distinguish between apparent solubility and equilibrium solubility. Apparent solubility refers to the solubility of a solute in a solvent system where insufficient time is allowed for the system to approach equilibrium, whereas equilibrium solubility is defined as the solute concentration capable of dissolving in a saturated solution at thermodynamic equilibrium.[43]

1.5. Chronic Kidney Disease-Associated Anemia

Chronic kidney disease (CKD) is a condition in which the structure and function of the kidney is affected. That said, the diagnosis of CKD is based on the finding of a chronic reduction in kidney function and structural damage to the kidneys for 3 months or more, where the best available indicator of overall kidney function is the glomerular filtration rate (GFR).[44] This indicator is important for classifying this disease into five phases, which are, more than 90 mL/min per 1-73 m^2 (phase 1), 60-89 mL/min per 1-73 m^2 (phase 2), 30-59 mL/min per 1-73 m^2 (phase 3), 15-29 mL/min per 1-73 m^2 (phase 4), and less than 15 mL/min per 1-73 m^2 (phase 5). When symptoms are severe, only dialysis and transplantation are effective treatments.[45]

Although the diagnosis of this disease is difficult, in developed countries, chronic kidney disease is associated with advanced age, obesity, diabetes, and hypertension, while in developing countries, it is associated with glomerular and tubulointerstitial diseases resulting from infections and exposure to drugs and toxins.[45]

The kidneys' inability to produce erythropoietin, a hormone that stimulates red blood cell production, means that patients suffering from chronic kidney disease can develop anemia. Anemia can occur at any stage of CKD and becomes more common as it progresses.[46] [47]

The current treatment for anemia in CKD focuses on the use of erythropoiesis-stimulating agents (erythropoietin analogues)[48] with intravenous iron supplementation, mainly in phase 5 of this disease, however, because there is a higher risk of death and major cardiovascular events when using erythropoietin analogues, the FDA has issued cautions concerning their use.[49]

The rising incidence of kidney failure and the early stages of chronic kidney disease, as well as the high costs (dialysis and transplantation) and insufficient treatment outcomes, pose a threat to public health on a global scale.[45]

Therefore, it is very important to find a solution to the treatment currently used for the anemia associated with CKD.

1.6. Roxadustat

Historically, the primary treatment for anemia in CKD patients has been the use of erythropoiesis-stimulating agents (ESAs), which stimulate the production of red blood cells. However, concerns about safety, cost, and variable responses have driven the search for novel therapeutic approaches. In recent years, a new class of drugs called hypoxia-inducible factor prolyl hydroxylase inhibitors (HIF-PHIs) has emerged as a promising alternative.[50,51]

Roxadustat (ROXA), Figure 3, also known as FG-4592, is a small molecule hypoxia-inducible factor (HIF) prolyl hydroxylase inhibitor that is administered orally.[52] It is approved for the clinical treatment of renal anemia in China, the European Union, Japan, South Korea, and Chile. This drug has shown good efficacy and safety in the treatment of dialysis and non-dialysis dependent patients with chronic kidney disease.[53] [54]

When compared to other CKD treatment alternatives, roxadustat has several advantages, such as the ability to be administered orally rather than intravenously or subcutaneously, which is more uncomfortable, and a greater ability to increase hemoglobin levels in a shorter period of time.[55]

ROXA presents itself as an effective alternative for the treatment of chronic kidney disease, however several trials are still ongoing. In addition, the solid behavior of this pharmaceutical product is poorly known, which makes it very important to study its solid forms. [56,57]

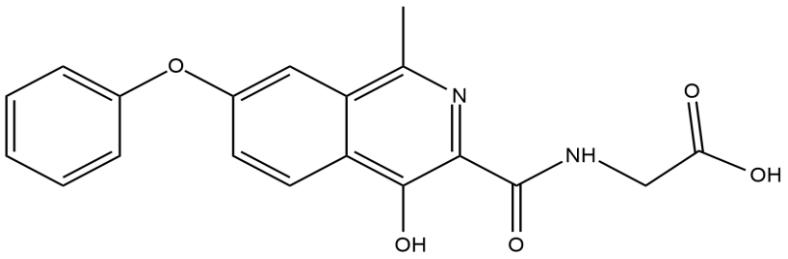

Figure 3 - Roxadustat molecular structure

1.6.1. Roxadustat Pharmacodynamics

Pharmacodynamics (PD) is the study of a drug´s molecular, biochemical, and physiologic effects on the human body. It studies the relationship between drug exposure (concentrations or dose) and pharmacologic or toxicologic responses. Understanding a compound's biochemical effect in the body as well as the molecular and cellular mechanisms behind the target pathology is crucial since it helps the development of more effective drugs and improves clinical studies. When it comes to its mechanism of action, roxadustat is a hypoxia-inducible factor (HIF) prolyl hydroxylase inhibitor.[55] HIFs are transcription factors that regulate expression of genes in response to reduced oxygen levels, including genes required for erythropoiesis and iron

metabolism. In normal oxygen concentrations, hypoxia-inducible factor prolyl hydroxylase (HIF-PH) hydroxylate the HIF-α subunit, resulting in its proteasomal degradation. In contrast, under conditions of low oxygen concentrations, the activity of HIF-PH decreases, allowing HIF to increase erythropoiesis in response to hypoxia.[52] Therefore, roxadustat is a very useful pharmaceutical active ingredient, since it reversibly binds and inhibits HIF-PH, reducing HIF-α degradation and improving HIF transcriptional activity, and consequently promotes the induction of target genes involved in erythropoiesis, increase haemoglobin levels, and reduce hepcidin levels in patients with chronic kidney disease-associated anemia.[53]

1.6.2. Roxadustat Pharmacokinetics

There is an increasing need to develop optimal drugs for different clinical challenges. The study and development of a drug is a very demanding process that requires a lot of time and costs. Developing the ideal drug is synonymous with being effective and safe. For this purpose, it is essential to know the pharmacokinetics (PK) and physicochemical properties of the substance in study.

While pharmacodynamics studies the effects of drugs on the body, pharmacokinetics is the study of how the body responds to administered substances throughout the entire period of exposure, concerning absorption, distribution, metabolism, and excretion (ADME), which is assessed through data collection in clinical pharmacology studies and helps explain the PK processes of a given drug.[58] Absorption refers to the transport from the route of administration into the systemic circulation and plays an important role in bioavailability, since the therapeutic effect is obtained from the fraction that is absorbed, during oral administration, as opposed to intravenous administration, in which drugs are transferred directly into the systemic circulation.[59] Once absorbed into the bloodstream, the drug can be transported throughout the body. This process is called distribution. The delivery of a drug from the bloodstream to the site of drug action depends on blood flow, capillary permeability, the degree of binding of the drug to blood and tissue proteins, and the relative lipid-solubility of the drug molecule.[59] Metabolism is a process where drugs undergo chemical changes in order to facilitate their excretion. Drugs metabolism can occur in different parts of the body, including the gastrointestinal tract, kidneys, plasma, and liver. Finally, when drugs are eliminated from the body, it is called excretion, and the most common route of elimination is the kidneys.[59,60]

Although many clinical trials are still underway with roxadustat, the pharmacokinetics of this drug is well characterized, with an apparent volume of distribution after oral administration of

22–57 L, apparent clearance of 1.2–2.65 L/h, and renal clearance of 0.030–0.026 L/h in healthy volunteers. The elimination half-life is 9.6–16 h. Plasma binding is 99% and the fraction eliminated by hemodialysis is 2.34%.[55]

1.7. Compounds used in single and multi-component systems investigation with Roxadustat

1.7.1. Selection process of coformers

The coformers shown in Figure 4 were selected and divided into four groups, considering their pharmacological interest and chemical structure.

In the carboxylic acids group, folic acid is a B-vitamin, which can interact with roxadustat by different kind of intermolecular interaction such as hydrogen bonding between the amine group of folic acid and roxadustat's oxygen functionalities. [61,62] All carboxylic acids have the potential of establishing hydrogen bonds with the aromatic nitrogen of roxadustat.[63,64] Citric acid is known as an excellent excipient, since it has antioxidant properties and it is used as a stabilizer agent in several drug formulations to increase their bioavailability[65]. Ascorbic acid is a vitamin C, known for its antioxidant properties.[66] Benzoic acid was used as a model compound.

Concerning the group of amides, benzamide, a simple amide compound, contains a benzene ring capable of interact with roxadustat´s aromatic rings and establish hydrogen bonding between its amide group and roxadustat´s oxygen functionalities.[67] Nicotinamide is a derivate of vitamin B3 that contains an amide group capable of participate in hydrogen bonding with roxadustat and a pyridine ring able to engage in π-π stacking interactions with roxadustat's aromatic rings as well as in COOH $\cdots N_{aromatic}$ intermolecular interactions.[68,69] Isonicotinamide, an isomer of nicotinamide, is able to have the same type of interactions with roxadustat as the last amide.[69,69] Finally, pyrazinamide is an important antitubercular drug, and, once again this amide could engage in π-π stacking interactions with roxadustat's aromatic rings and establish hydrogen bonds with roxadustat through the amide group.[70]

Caffeine and theophylline are both methylxanthines that share structural similarities and possess the potential to interact with roxadustat through forming different synthons. The first xanthine is a central nervous system stimulant and a muscle relaxant that is frequently included in the formulation of analgesics.[71] Caffeine has a nitrogen atom in the imidazole group and two oxygen atoms in the carbonyl groups that can be used as targets for hydrogen bonds. The second xanthine,[72] theophylline is a derivative of caffeine and is used in the treatment of asthma and cardiopulmonary disease.[73] The presence of hydrogen bond donor and acceptor groups in theophylline's structure suggests the potential for hydrogen bonding with roxadustat's functional groups, however the presence of both donor and acceptor groups in this molecule adds an extra element of complexity to the synthesis of cocrystals.[74]

The fourth group involves amino acids and pyridoxine. L-histidine, an essential amino acid, contains an imidazole side chain that can engage in hydrogen bonding and π-π stacking interactions with roxadustat.[75] Cysteine, a sulfur-containing amino acid, is known for its ability to form disulfide bonds and participate in redox reactions[75]. Tryptophan, an aromatic amino acid, features a highly conjugated ring system that can participate in π-π stacking interactions with the API. Pyridoxine, also known as vitamin B6, is a water-soluble vitamin involved in various enzymatic reactions.[76] Its pyridine ring could potentially engage in π-π stacking interactions with roxadustat's aromatic rings, as well as in $COOH\cdots N_{aromatic}$ intermolecular interactions.[77]

The last group of coformers contains three molecules, namely 1,2 Bis (4-pyridyl) ethane, 4,4 bipyridyl and pyrazine. These are model compounds, often used in cocrystals screening, that share the same kind of functional groups.[78] 4,4 bipyridyl is known for its ability to form coordination complexes due to its nitrogen donor atoms. Its aromatic rings could potentially stack with aromatic rings in roxadustat through π-π interactions and the nitrogen atoms in the ligand might also form hydrogen bonds with roxadustat's functional groups.[78] Lastly, pyrazine, a six-membered aromatic ring with two nitrogen atoms, has the potential to participate in π-π stacking interactions with aromatic rings in roxadustat and the nitrogen atoms could also engage in hydrogen bonding interactions with roxadustat's functional groups.[79]

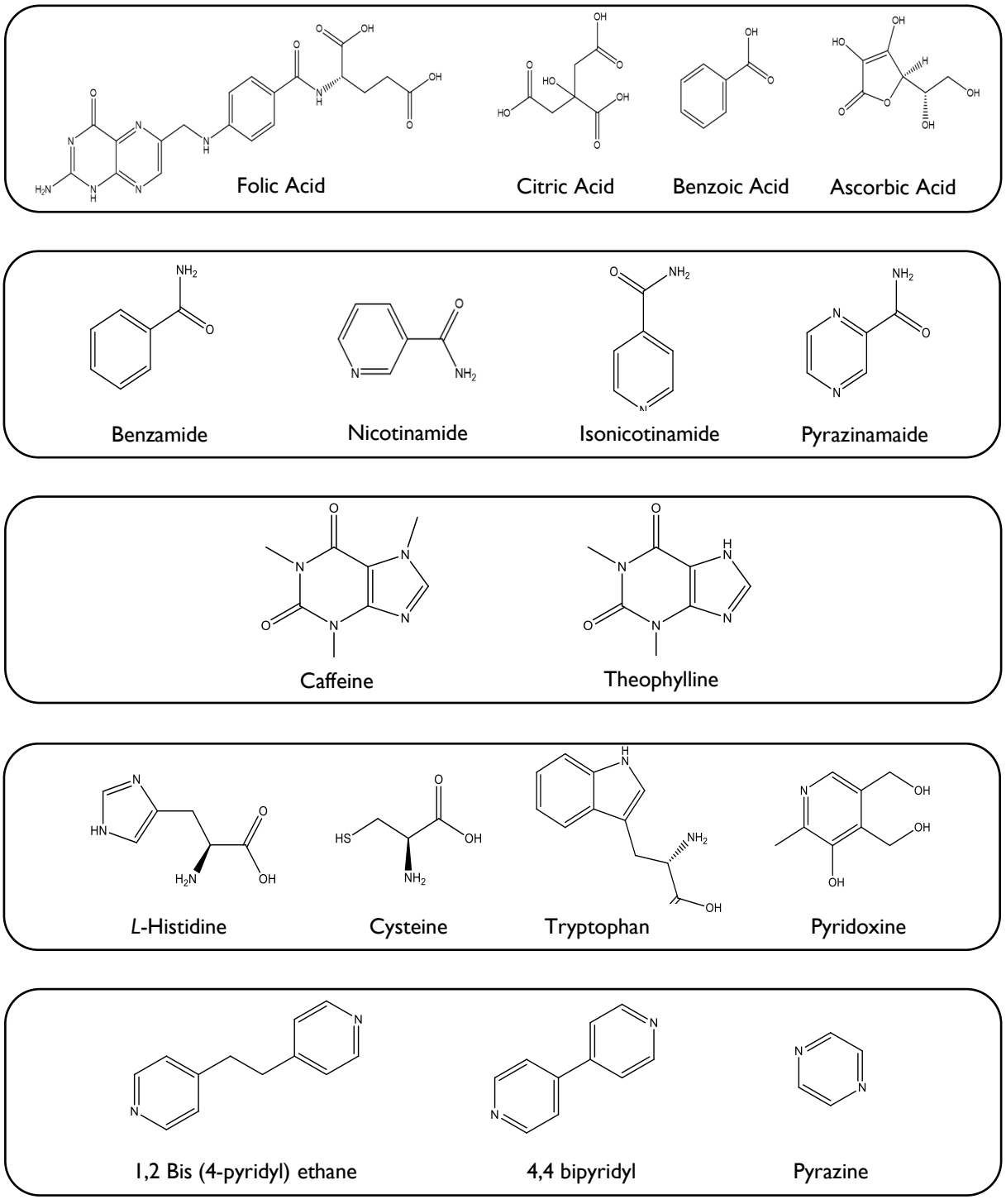

Figure 4 - Compounds used, in this work, as coformers in studies with ROXA

1.8. Objective

The development of more effective and safer pharmaceutical forms is a major scientific challenge, since it is necessary to know the most suitable solid form of the active substance, as well as the most suitable excipients and manufacturing processes in the development of a drug. To this end, it is important to first detail the physicochemical characteristics of the API, long before its pharmacological evaluation.

Roxadustat is a drug that presents itself as a good alternative to the current treatment of chronic kidney disease associated anemia, however, there are still many physicochemical characterization trials in progress, which makes this drug a very interesting research target for preformulation studies.

This work aims to perform relevant preformulation studies on roxadustat. The solid state behavior of pure roxadustat and the screening and characterization of roxadustat containing multicomponent solid forms is carried out. The solubility of promising solid forms, from a pharmaceutical point of view, is also evaluated in aqueous HCl simulating the pH of the medium where this active substance is absorbed (stomach: pH≈1-3).

2. MATERIALS AND METHODS

2.1. Materials

Table I - Chemical materials used, and respective abbreviation/chemical formula, supplier, molecular mass, and purity

Chemical Material	Abbreviation	Supplier	M (g/mol)	Purity / %
Roxadustat	ROXA	Xiao Fu Trading Co. Lda	352.3	≥ 98 %
1,2-Bis(4-pyridyl) ethane	BPA	Sigma-Aldrich	184.24	99%
Nicotinamide	NICO	Sigma-Aldrich	122.12	≥ 99.5 %
Isonicotinamide	ISO	Sigma-Aldrich	122.13	99%
Benzamide	BENZ	Sigma-Aldrich	121.140	99.9%
Pyrazinamide	PZA	Fluka	123.12	≥ 99 %
Pyrazine	PYZ	Sigma-Aldrich	80.09	≥ 99 %
Caffeine	CAF	Sigma-Aldrich	194.19	≥ 99 %
Theophylline	THEO	Sigma-Aldrich	180.16	99%
4,4 -Bipyridyl	BPY	Fluka	156.19	≥ 99 %
Folic acid	FA	Sigma-Aldrich	441.40	≥ 97 %
Citric Acid	CIA	BLDpharm	192.12	98%
Benzoic acid	BZA	Riedel-de Haën	122.12	99.9%
Ascorbic acid	ACA	Merck	176.12	99%
Cysteine	CYS	Sigma-Aldrich	121.16	≥ 98 %
L-histidine	HIS	Sigma-Aldrich	155.15	≥ 99 %
Tryptophan	TRP	Sigma-Aldrich	204.23	≥ 99.5 %
Pyridoxine	PYX	Sigma-Aldrich	169.18	≥ 98 %
Ethanol	EtOH	Fisher Chemical	46.07	99.8%
Methanol	MeOH	Fluka	32.04	99.8%
Hydrochloric acid	HCl	Fluka	36.46	37%
Sodium hydroxide	NaOH	J.T Baker	40.00	98.7%

2.2. Methods

2.2.1. Mechanochemistry (LAG and NG)

Mechanochemistry is an efficient method for the synthesis of multicomponent systems induced by external mechanical force.[80] This technique can be used either manually or using mills, for instance ball mills, in which the vessels are shaked at a specific frequency for a specific period of time, causing the balls to collide with the sample, inside the vessels.[81]

Neat grinding (NG) is the simplest process of cocrystallization by mechanochemistry, however, in the absence of solvent, the reaction is not always effective.[82] Liquid assisted grinding (LAG) proved to be a good alternative, since the addition of catalytic amounts of solvent can accelerate the reaction and obtain a more crystalline product.[80,81] Mechanochemistry by liquid assisted grinding can, however, lead to the formation of solvates,.[81,82]

Mixtures were prepared by ball milling, using a Retsch MM400 mill with two stainless-steel grinding balls (7 mm diameter) in 10 mL stainless-steel jars.

Neat grinding was used for amorphous and coamorphous synthesis, while liquid assisted grinding took place to produce cocrystals, with ethanol as the reaction enhancing solvent.

The samples, with a total mass of 100 mg, were grinded at a frequency of 30 Hz, for 30 and 60 min, according to the desired results.

2.2.2. Differential Scanning Calorimetry (DSC)

Differential scanning calorimetry provides a calorimetric analysis of the samples under study, measuring the differential heat flow between a sample and reference material, allowing to study its thermal response to temperature changes.[83] This technique allows the identification of various events such as melting point, recrystallization, polymorphic and glass transition and chemical reactions.

There are two different types of DSC. In this work, power compensation DSC was used as a method of characterization. In this type of DSC, the sample and the reference are placed in two different thermally isolated with controlled temperature ovens. This calorimeter measures the difference in heat flux (dQ/dt) between the sample and the reference as a function of temperature. The two pans are subjected to a program of controlled temperature variation and, if temperature differences are detected between the sample and the reference, the energy supplied is adjusted to bring them back into thermal equilibrium.[84]

Energy absorption is recorded as endothermic peaks (positive sign) and release as exothermic peaks (negative sign). Therefore, during an endothermic event the DSC supplies energy to the sample.[84,85] The heating rate influences the nature of the thermoanalytical curve - low heating rates result in high resolution and low sensitivity, so low energy events may not be detected.[84] In the study of new multicomponent systems, it is important to perform a calorimetric analysis by DSC.

The equipment used was a DSC7 power compensation calorimeter from Perkin Elmer, with an intracooler unit at - 20 °C and a N_2 purge with a flow rate of 20 mL/min. Samples weighting 1.5 to 2.5 mg were prepared in 10 µl hermetically sealed aluminium pans and scanning rates of β = 10 °C/min and β = 20 °C/min were used.

2.2.3. Fourier Transform Infrared Spectroscopy with ATR module (FTIR-ATR)

FTIR is a spectroscopy technique which allows to directly monitor the vibrations of functional groups that characterize the molecular structure of the compounds under study. It is based in the interaction of electromagnetic radiation within the infrared region with the sample.[86]

The main component of FTIR is the interferometer, which acts as a beam splitter. In this way, half of the beam coming from the source is incident on a fixed mirror and the other half on a moving mirror and is reflected, creating constructive and destructive interferences. The already modulated radiation passes through the sample which selectively absorbs it. Subsequently, the detector records the radiation in the form of an interferogram and the information contained within it is translated into a spectrum using the Fourier transform.[86]

ATR module was used because it allows samples to be analysed directly, without causing changes in their solid structure.

Solid samples infrared spectra were collected with from a Thermo Nicolet IR380 spectrometer with ATR Diamond accessory with a spectral resolution of 2 cm^{-1} and 32 scans.

2.2.4. X-ray Powder Diffraction (XRPD)

XRPD is a diffraction technique used to detect and quantify molecular order in any system. It is based on the measurement of X-ray scattering from the entire sample including the crystalline and amorphous phase.[87,88]

This method is extremely helpful in characterizing solid forms, such as cocrystals, coamorphous, and amorphous materials. XRPD diffractograms of amorphous solids show no

diffraction peaks, due to the lack of crystal lattice, while crystalline forms show strong diffraction peaks in their diffractograms.[89]

X-ray beams generated by a cathode ray tube are filtered to produce monochromatic radiation and collimated. When they reach the sample, they may be reflected or may be diffracted. The diffracted beams generate constructive interference, creating a unique pattern for each sample that depends on the density of the atoms and their organization.[88]

X-ray diffraction follows Bragg's Law:

$$n\lambda = 2d \sin\theta$$

- n is an integer;
- λ is the wavelength of the X-rays;
- d is the interplanar spacing generating the diffraction;
- ϑ is the diffraction angle.[88]

Diffractograms were obtained in a Rigaku's MiniFlex 600 equipment with the D/teX Ultra detector. Data were acquired between 3-40° at a speed of 5°/min and the samples were prepared in a silicon sample holder with a cavity to place the sample of 5.0 mm in diameter and 0.1 mm deep.

2.2.5. Saturation Shake-Flask Method

Saturation shake-flask method is used to determine equilibrium solubility. This method consists of preparing, in a flask, a suspension of the solid in the chosen medium without the need for measuring the quantity of solid or solvent. It is important that at least triplicate essays are carried out.[43,90]

To achieve equilibrium, the solutions must be constantly agitated for a certain period of time at a constant temperature. Samples should be analysed more than once for different time periods to determine the concentration of solute and assure that the equilibrium has been reached. These analyses can be performed using UV-Vis spectrometry or by liquid chromatography methods.

In this work, the saturation flask method was used to study the equilibrium solubility of roxadustat, alone, from two cocrystals (ROXA+CAF and ROXA+NICO) and from a coamorphous (ROXA+PYX). The choice of these two cocrystals and the coamorphous was due to the fact that they all have pharmacological interest.

Three saturated solutions were prepared for each of the three samples. The solvent chosen for the solutions was aqueous HCl to simulate the pH of the medium where the active substance in study is absorbed (stomach: pH≈1-3). After preparing these suspensions, they

were stirred constantly for 48h at a constant temperature of 37°C and then aliquots of the solutions were filtered and diluted in an alkaline medium (NaOH 10^{-3} M) in order to measure absorbance of a single roxadustat species (fully deprotonated) at 360 nm, by UV-Vis spectometry.[91] This analysis was performed in a Shimadzu UV-1800 spectrophotometer using Quartz cuvettes with an optical path of 1 cm. These values, after preparing a calibration curve, were then used to calculate the concentrations of roxadustat in the final solutions for the different samples.

3. RESULTS AND DISCUSSION

3.1. Roxadustat: characterization of the starting compound

The thermal behaviour of the starting roxadustat sample was characterized by differential scanning calorimetry as shown in Figure 5.

The heating curve of the starting compound shows a narrow endothermic peak. The melting temperature and enthalpy of fusion are in accordance with the literature.[92] T_{fus} = (223,5 ± 0,6) °C and $\Delta_{fus}H$ = (47,0 ± 1,0) kJ.mol^{-1}.

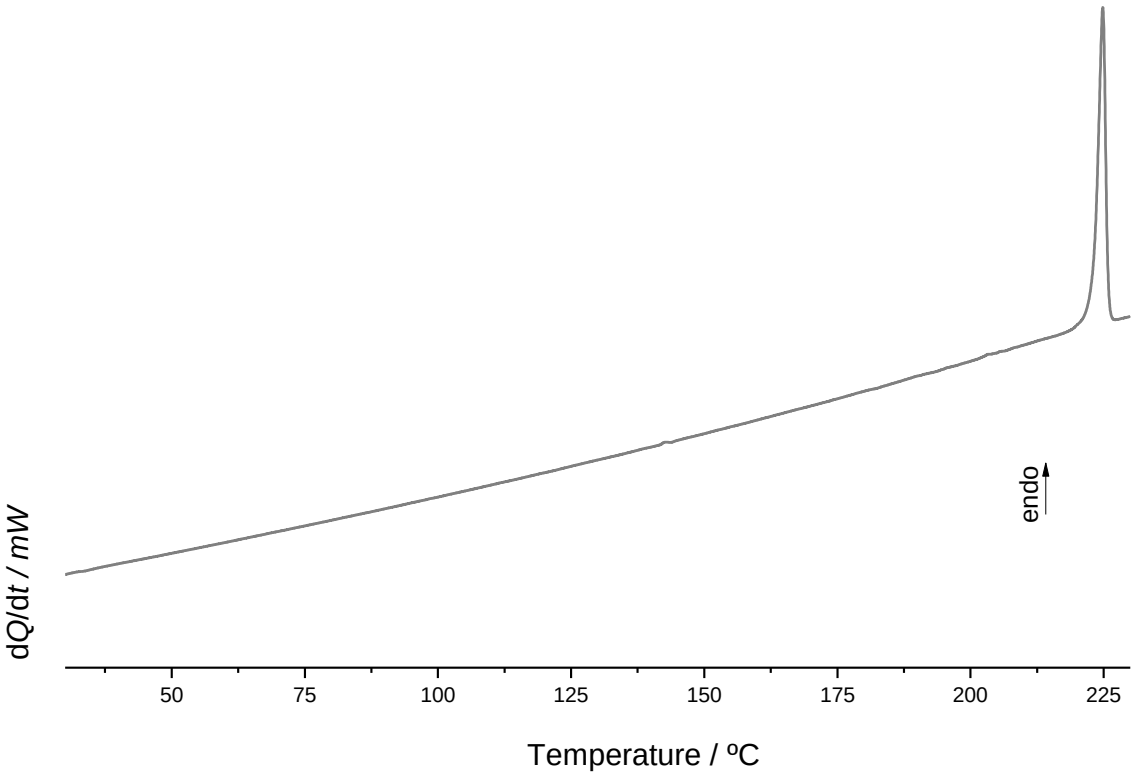

Figure 5 - DSC heating curve of the starting sample of roxadustat, β = 10 °C/min

Figure 6 shows the infrared spectrum of the commercial roxadustat sample. The N-H stretching vibration is found at 3360 cm^{-1}, between 3200-2400 cm^{-1} there is the band characteristic of the OH stretching of the carboxylic group, at 1700 cm^{-1} - the band characteristic of the stretching of the C=O group. Both 1275- 1200 cm^{-1} and 1075-1020 cm^{-1} bands are characteristic of aromatic esters and the band at 941 cm^{-1} refers to O-H...O deformation, characteristic of carboxylic acid dimers.

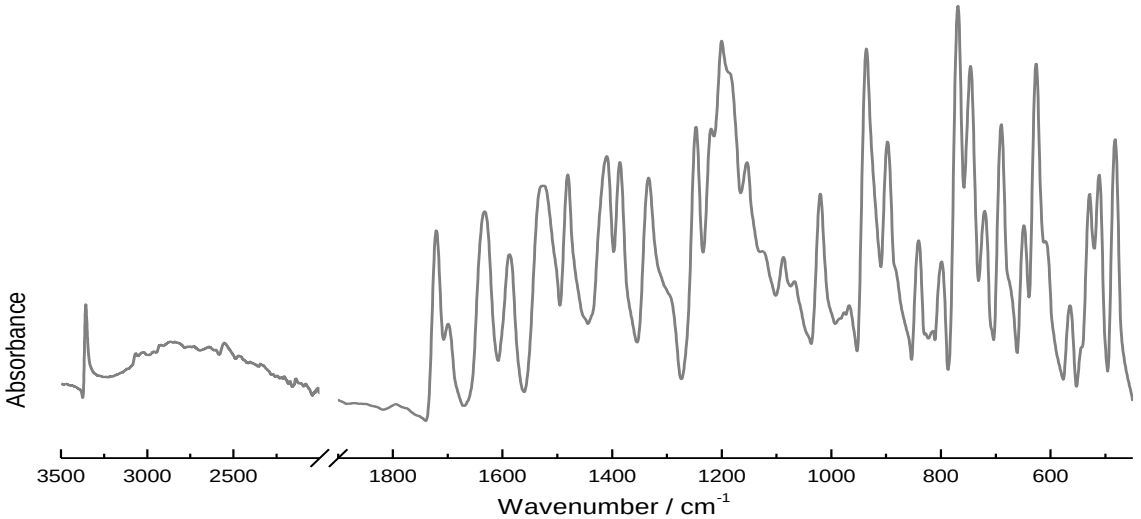

Figure 6 - FTIR spectrum of the starting sample of roxadustat

The commercial sample of roxadustat was also subjected to XRPD analysis for better characterization - shown in Figure 7. It shows the characteristics reflections of roxadustat obtained for the CCDC 1469842 structure, solved in our laboratory.[92]

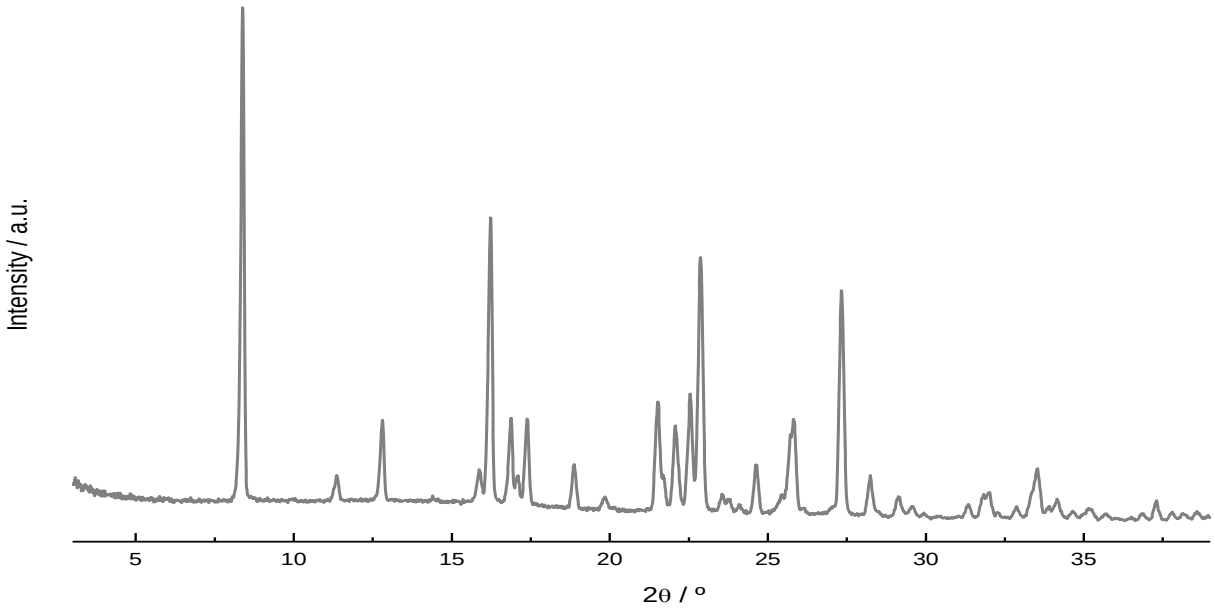

Figure 7 - XRPD diffractograms of the starting sample of roxadustat

3.1.1. Roxadustat amorphization by neat grinding

Roxadustat amorphization was studied with mechanochemistry, by neat grinding (NG). NG was performed at 30 Hz for 30 minutes and 60 minutes. From the analysis of the diffractograms in Figure 8, it can be concluded that 30 minutes was not enough to amorphized roxadustat. While two reflections due to crystalline roxadustat were still noticeable in the attempted amorphization in the 60 minutes condition, this was very close to complete amorphization.

Figure 9 shows the DSC heating curve of the sample obtained at 30 Hz for 60 minutes with a glass transition at T = 54.3 °C, followed by crystallization and melting temperature at T = 217.7 °C, enthalpy of fusion ΔH = 122.6 kJ/mol.

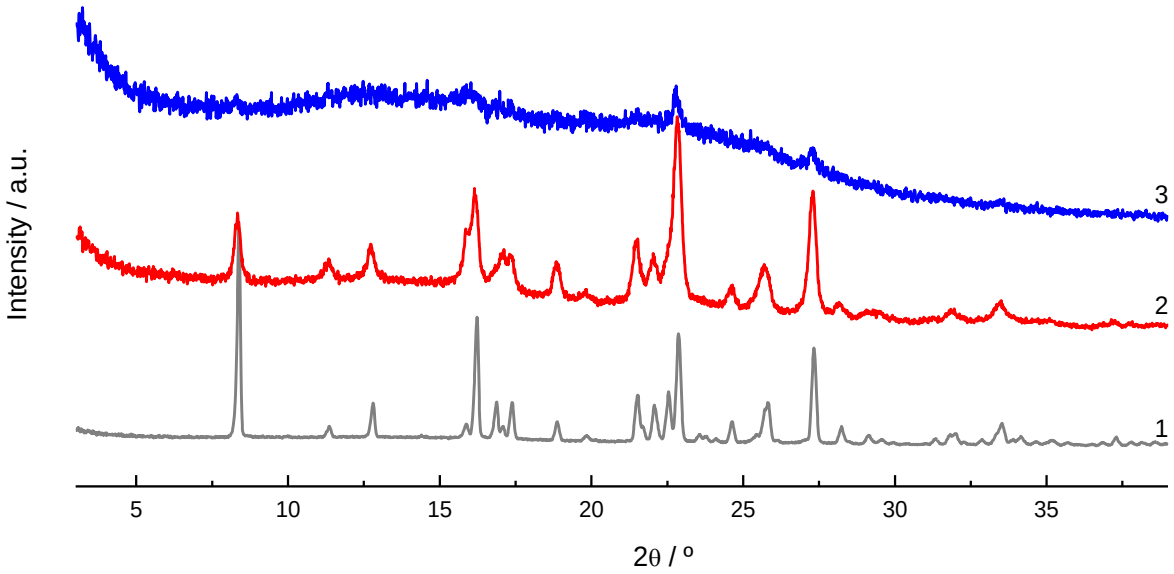

Figure 8 - XRPD diffractograms: 1. starting sample of roxadustat; 2. roxadustat NG - 30 Hz for 30 minutes; 3. roxadustat NG - 30 Hz for 60 min

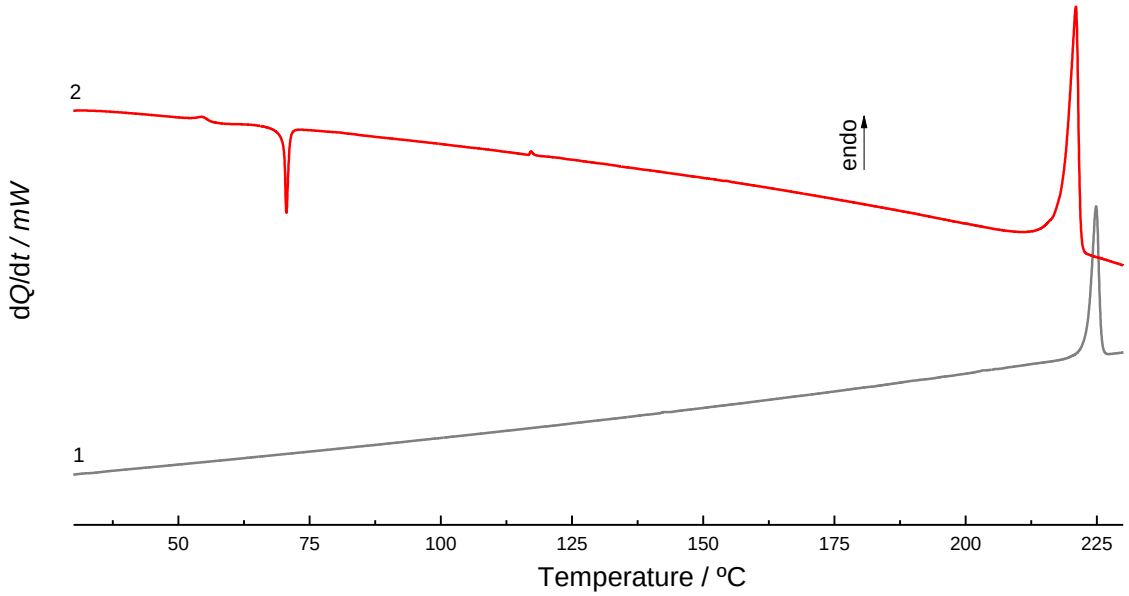

Figure 9 - DSC heating curves: 1. starting sample of roxadustat; 2. roxadustat NG - 30 Hz for 60 min; β = 10 °C/min

3.2. Investigation of roxadustat cocrystals and coamorphous phases

The investigation of cocrystals and coamorphous phases of roxadustat was carried out by mechanochemistry, liquid assisted grinding (LAG) and neat grinding (NG). Different coformers was used attempting to form cocrystals and coamorphous of roxadustat. Different molar ratios were tested for binary mixtures of this API and coformers, selected in order to be able to form different heterosynthons with roxadustat or due to their pharmaceutical properties.

NG was mainly used to form coamorphous forms, while LAG took place to produce cocrystals, with 10 µl of ethanol as the reaction enhancing solvent.

For each mixture, analyses of the solids obtained were carried out for their characterization, using methods such as DSC, FTIR-ATR and XRPD.

3.2.1. Roxadustat + Carboxylic Acids

Roxadustat + Folic Acid

Equimolar mixtures of roxadustat and folic acid were prepared by neat grinding at 30 Hz during 30 min in order to form a coamorphous compound. Figure 10 shows the XRPD diffractograms of the solid mixture, roxadustat + folic acid (1:1), as well as, of the pure compounds, roxadustat and folic acid.

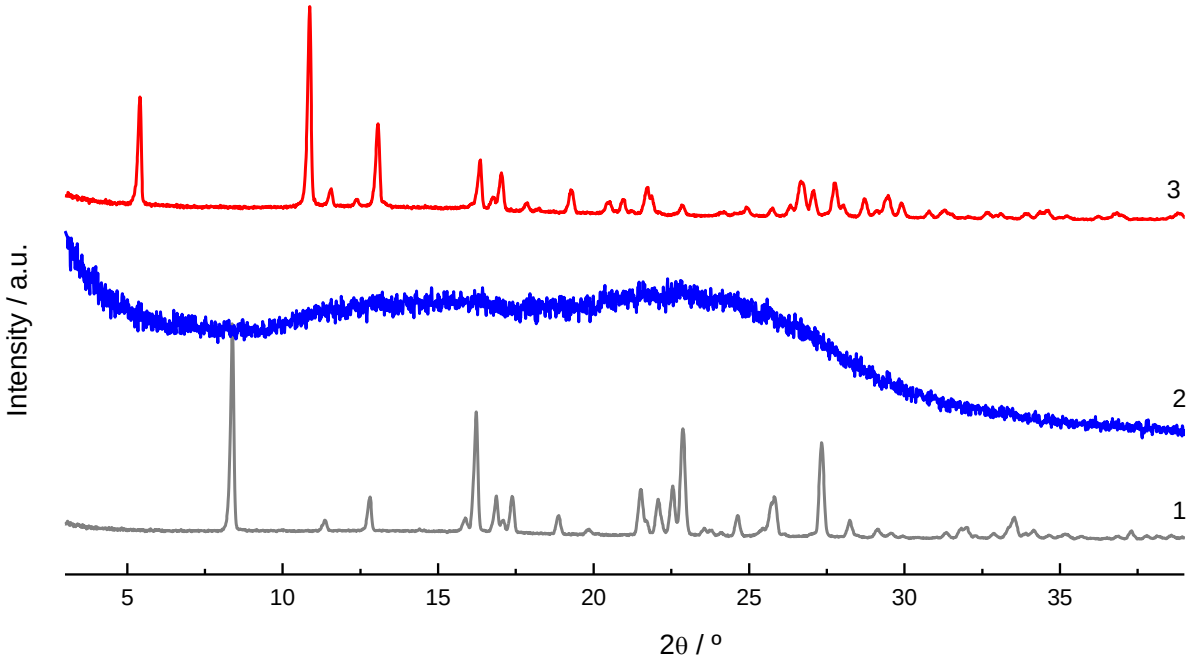

Figure 10 - XRPD diffractograms: 1. roxadustat; 2. roxadustat + folic acid (1:1) by NG; 3. folic acid

From the analysis of the diffractograms in Figure 10, it can be concluded that a coamorphous solid was formed by the mixture of roxadustat + folic acid (1:1), since curve 2 shows a characteristic amorphous halo and no crystal reflections. The solid mixture has also been analysed by thermal analysis, DSC, and infrared spectroscopy, FTIR-ATR. Figure 11 shows the thermograms of the mixture obtained and of the pure compounds.

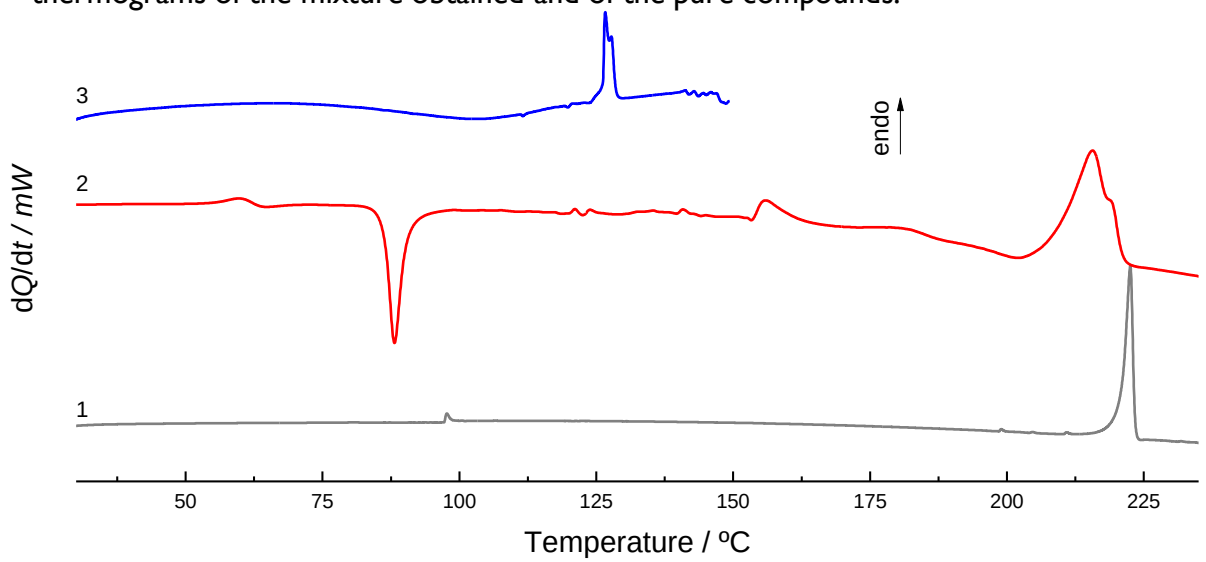

Figure 11 – DSC heating curves: 1. roxadustat; 2. roxadustat + folic acid (1:1) by NG; 3. folic acid; β = 10 °C/min

When analysing the DSC curves, it can be observed, in curve 2, a typical single glass transition, at *Tg* = 58.2 °C followed by crystallization, common in coamorphous DSC curves. The infrared spectrum 2 , represented in Figure 12, shows a typical spectrum of a coamorphous compound, since its bands are broader compared to the spectra of the pure crystalline compounds, roxadustat and folic acid.

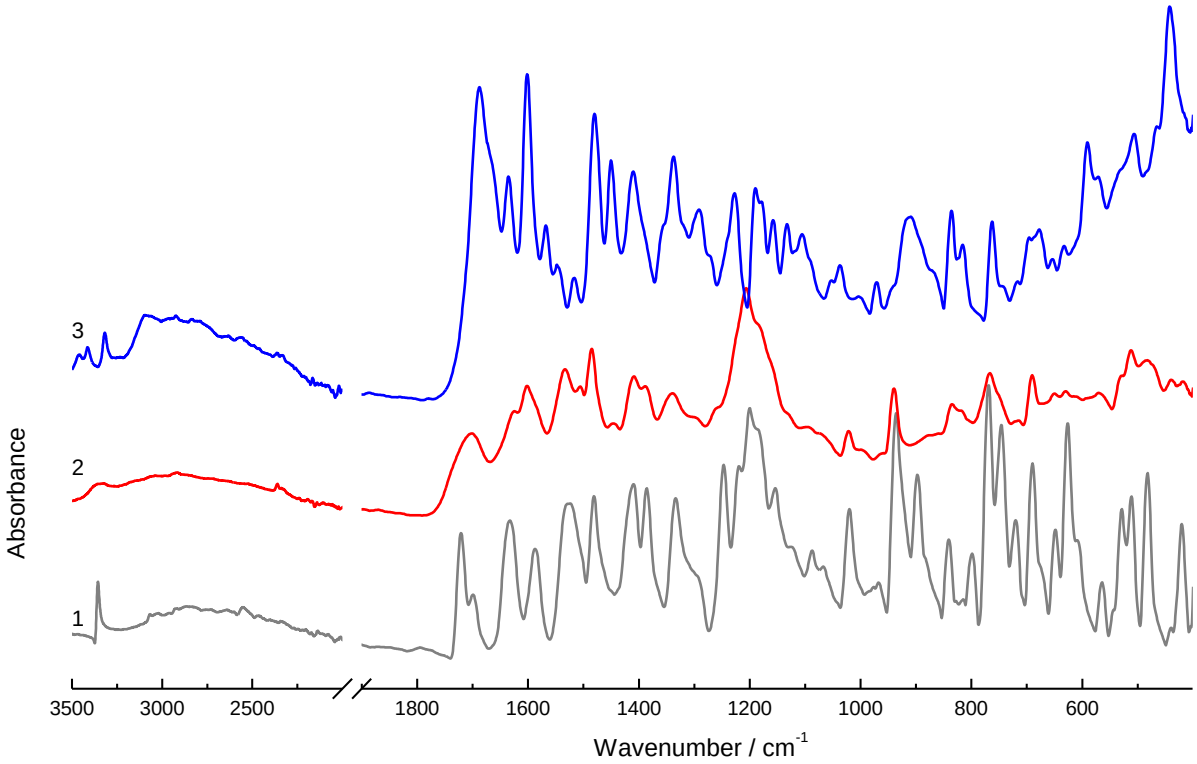

Figure 12 - FTIR spectra: 1. roxadustat; 2. roxadustat + folic acid (1:1) by NG; 3. folic acid

Roxadustat + Citric Acid / Roxadustat + Benzoic Acid / Roxadustat + Ascorbic Acid

The other carboxylic acids (citric acid, benzoic acid, and ascorbic acid) were also subjected to mechanochemistry, but unlike folic acid, their solid mixtures with roxadustat were prepared by liquid assisted grinding at 30 Hz for 30 min. Mixtures in 1:1 molar ratio and 2:1 and 1:2 ratios, were analysed.

The following graph, Figure 13, shows the diffractograms obtained by XRPD of the solid mixtures with the coformers mentioned above in a molar ratio of 1:1. By analysing it, it can be concluded that there was no association between these coformers and the API under study, since the diffractograms of the mixtures are the combined sum of the roxadustat and coformer used, respectively. The same results were obtained for the other proportions studied.

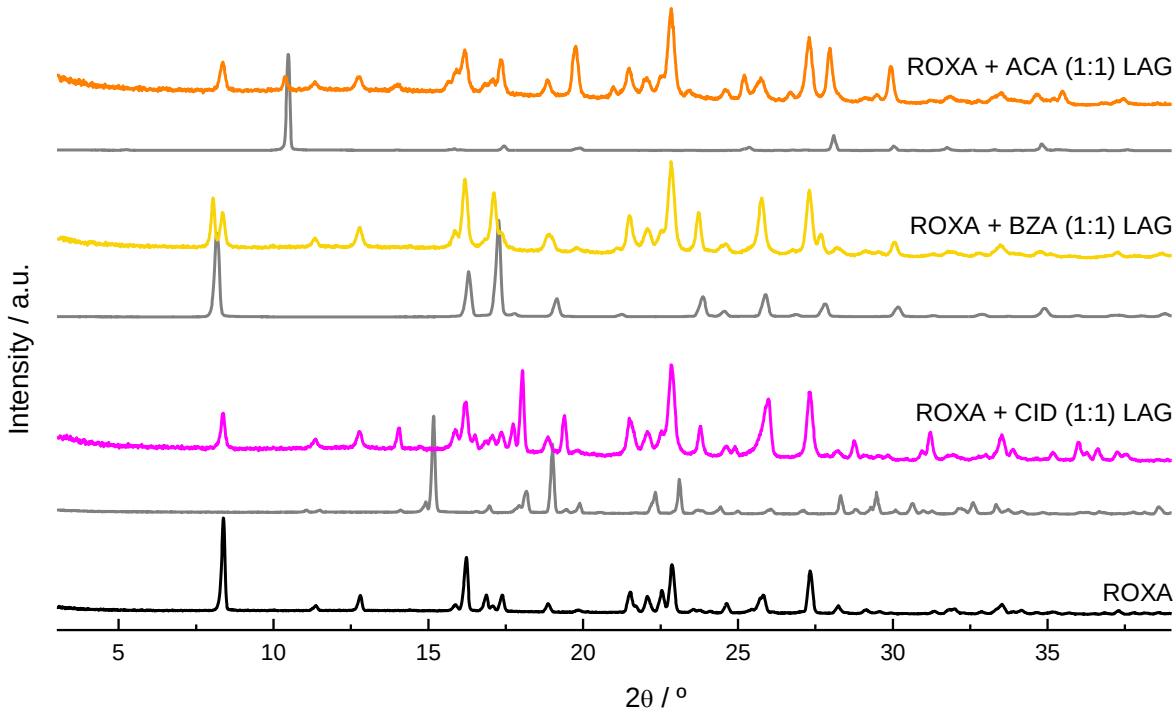

Figure 13 - XRPD diffractograms; roxadustat (black line), coformers (grey line) and respective solid mixtures

3.2.2. Roxadustat + Amides

Roxadustat + Benzamide

Different molar ratios of the roxadustat + benzamide mixture were prepared by liquid assisted grinding at 30 Hz for 30 min, with ethanol as the reaction enhancing solvent. The following graphs, Figures 14 to 16, show the analysis of a (1:1) roxadustat + benzamide cocrystal formed.

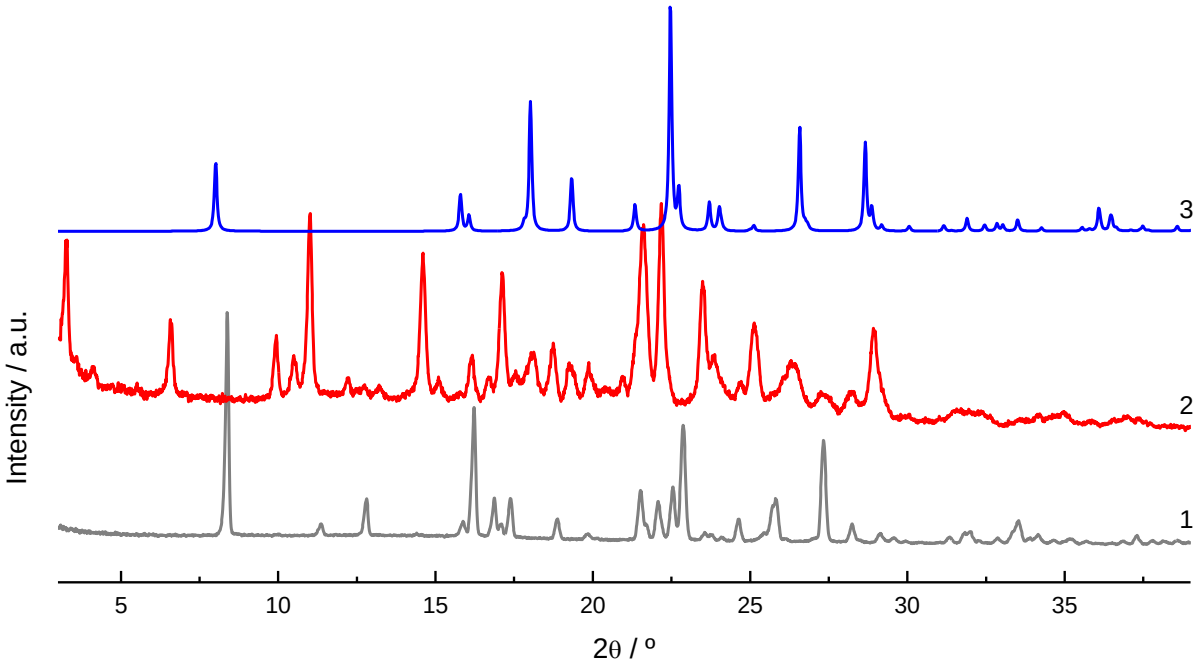

Figure 14 - XRPD diffractograms: 1. roxadustat; 2. roxadustat + benzamide (1:1) by LAG; 3. benzamide

The analysis of the resulting solid by XRPD, Figure 14, revealed some differences from the starting compounds, suggesting cocrystallization occurred. New reflections appear at 2ϑ = 3.3°, 6.6°, 14.6° and 23.5°, while characteristic reflections of both starting compounds are missing (e.g., 2ϑ = 8.4° and 22.8° for roxadustat and 2ϑ = 8.0° and 22.5°, for benzamide). This system was also studied by DSC and FTIR-ATR to prove the formation of a new cocrystal from the equimolar mixture, shown in Figure 15 and 16, respectively.

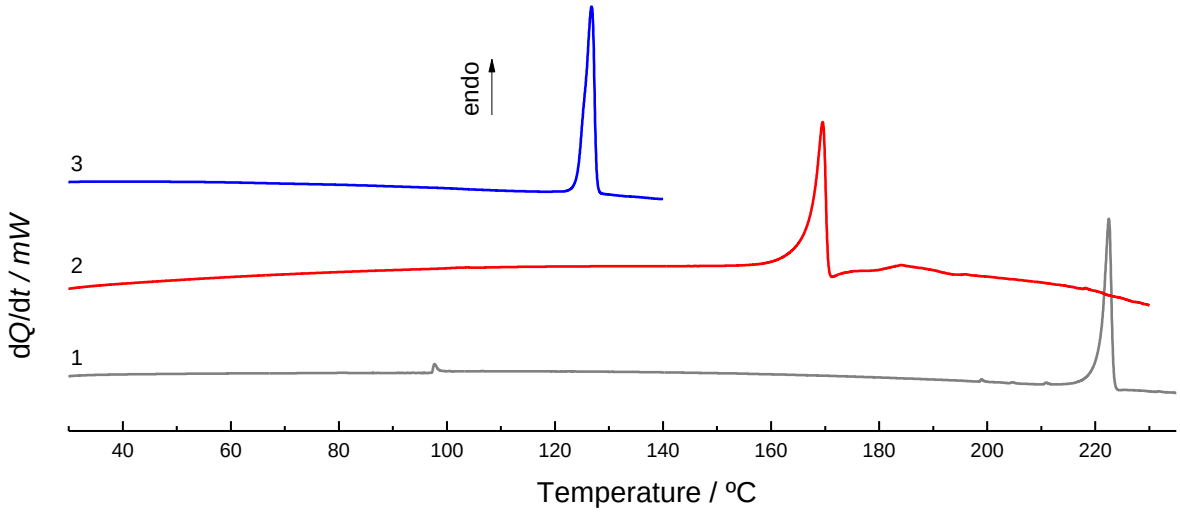

Figure 15 – DSC heating curves: 1. roxadustat; 2. roxadustat + benzamide (1:1) by LAG; 3. benzamide; β = 10 °C/min

DSC curves represented in Figure 15 revealed that the sample in a 1:1 molar ratio corresponds to the pure cocrystal. The DSC curve presents a single endothermic event, fusion at *T* = 166 °C, which is situated in the middle of both API and coformer fusion temperature values, which confirms the formation of a new solid form.

FTIR-ATR spectra, shown in Figure 16, exhibit significant differences between the cocrystal and the pure compounds.

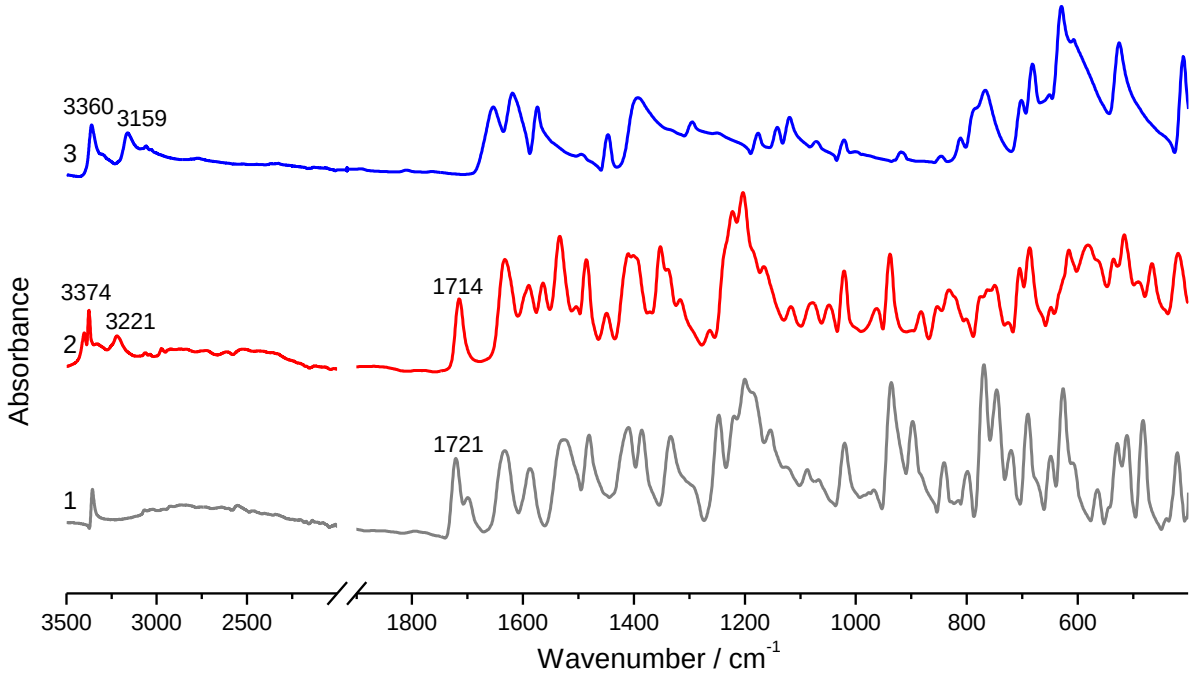

Figure 16 - FTIR spectra: 1. roxadustat; 2. roxadustat + benzamide (1:1) by LAG; 3. benzamide

The asymmetric elongation of NH_2, which in the spectrum of benzamide appears at 3360 cm^{-1}, is displaced to 3374 cm-1 in the spectrum of the mixture. The symmetrical elongation of NH_2 shifts from 3159 cm-1 in the benzamide to 3221 cm^{-1} in the mixture. It is also possible to observe the shift in the elongation of the C=O group, which in roxadustat is at 1721 cm^{-1} and in the mixture at 1714 cm^{-1}.

Roxadustat + Nicotinamide

Different molar ratios of roxadustat and nicotinamide were studied by liquid-assisted grinding under the same conditions as for the previously presented system. Nicotinamide was the only other amide studied in this work able to form a cocrystal in an equimolar mixture with roxadustat.

Based on the analysis of the diffractograms in Figure 17, the solid mixture of ROXA + NICO (1:1) shows a lot of different reflections when compared to the pure compounds: 2ϑ = 6.1°, 10.8°, 14.2° and 17.4°. The thermal behavior of this system was also studied by DSC.

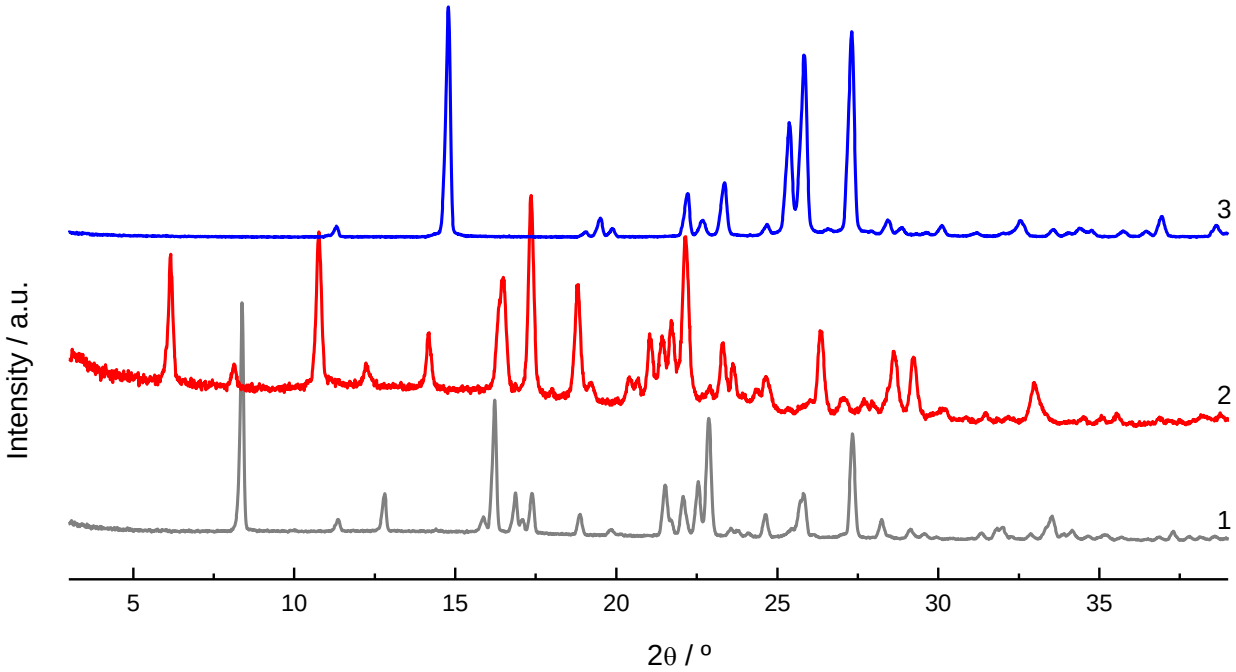

Figure 17 – XRPD diffractograms: 1. roxadustat; 2. roxadustat + nicotinamide (1:1) by LAG; 3. nicotinamide

Again, Figure 18 shows that the solid mixture under study melts at *T* = 148 °C , between the melting temperatures of the pure compounds.

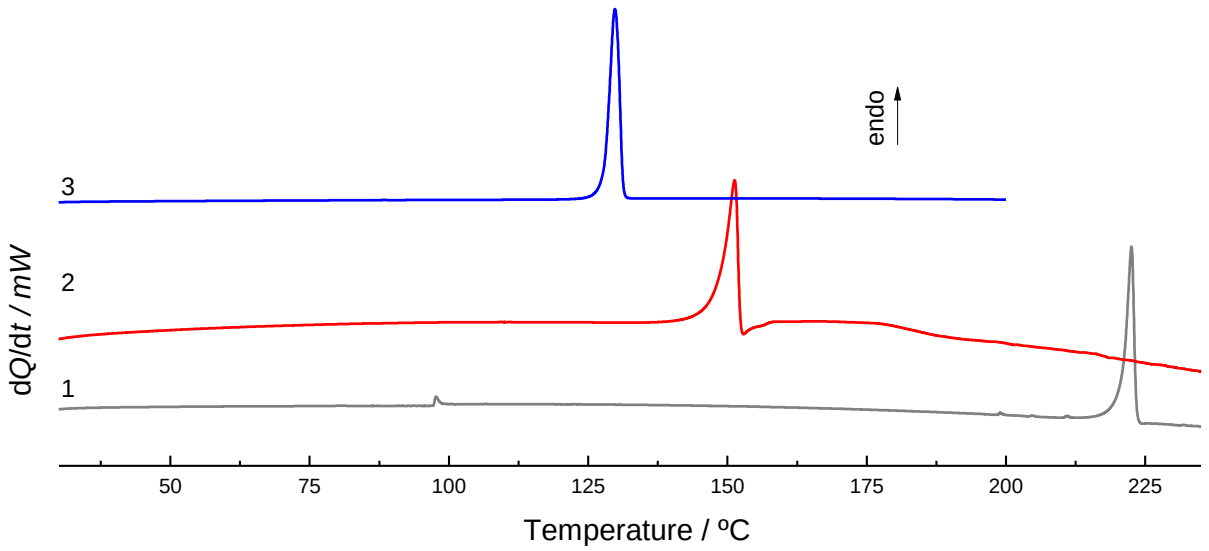

Figure 18 - DSC heating curves: 1. roxadustat; 2. roxadustat + nicotinamide (1:1) by LAG; 3. nicotinamide; β = 10 °C/min

Infrared spectroscopy, FTIR-ATR, was also used to study this solid mixture. As shown in figure 19, the spectrum of the pure cocrystal differs from that of pure compounds. The asymmetric elongation of NH_2, which in the spectrum of nicotinamide appears at 3358 cm^{-1}, is displaced to 3374 cm-1 in the spectrum of the mixture. The symmetrical elongation of NH_2 shifts from 3146 cm-1 in the nicotinamide to 3179 cm^{-1} in the mixture. It is also possible to observe the shift in the elongation of the C=O group, which in roxadustat is at 1721 cm^{-1} and in the mixture at 1725 cm^{-1}.

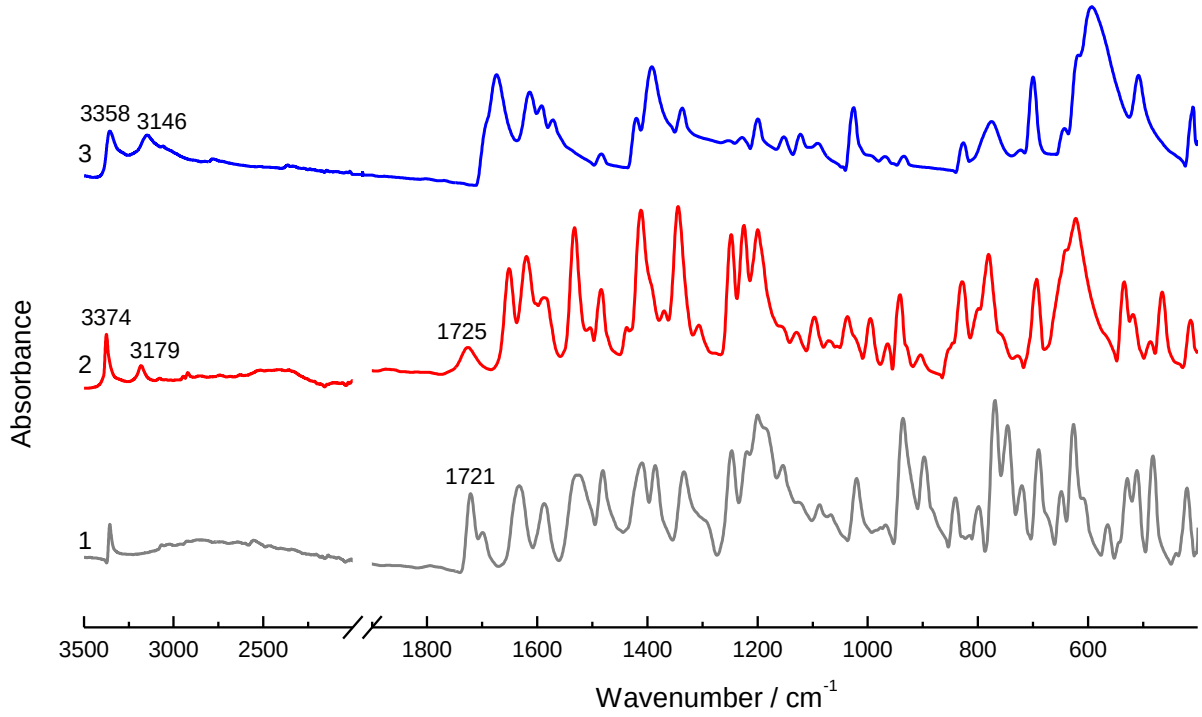

Figure 19 - FTIR spectra 1. roxadustat; 2. roxadustat + nicotinamide (1:1) by LAG; 3. nicotinamide

Roxadustat + Isonicotinamide / Roxadustat + Pyrazinamide

Mixtures of different molar ratios of other amides (isonicotinamide and pyrazinamide) and roxadustate were also studied (1:1, 2:1 and 1:2) by mechanochemistry with liquid assisted grinding at 30 Hz for 30 min, although only the 1:1 molar ration is shown in Figure 20.

From the analysis of the diffractograms represented in Figure 20, there was no association between isonicotinamide and roxadustat or pyrazinamide and roxadustat. The diffractograms of the mixtures are simply the sum of the pure compound and the coformers used.

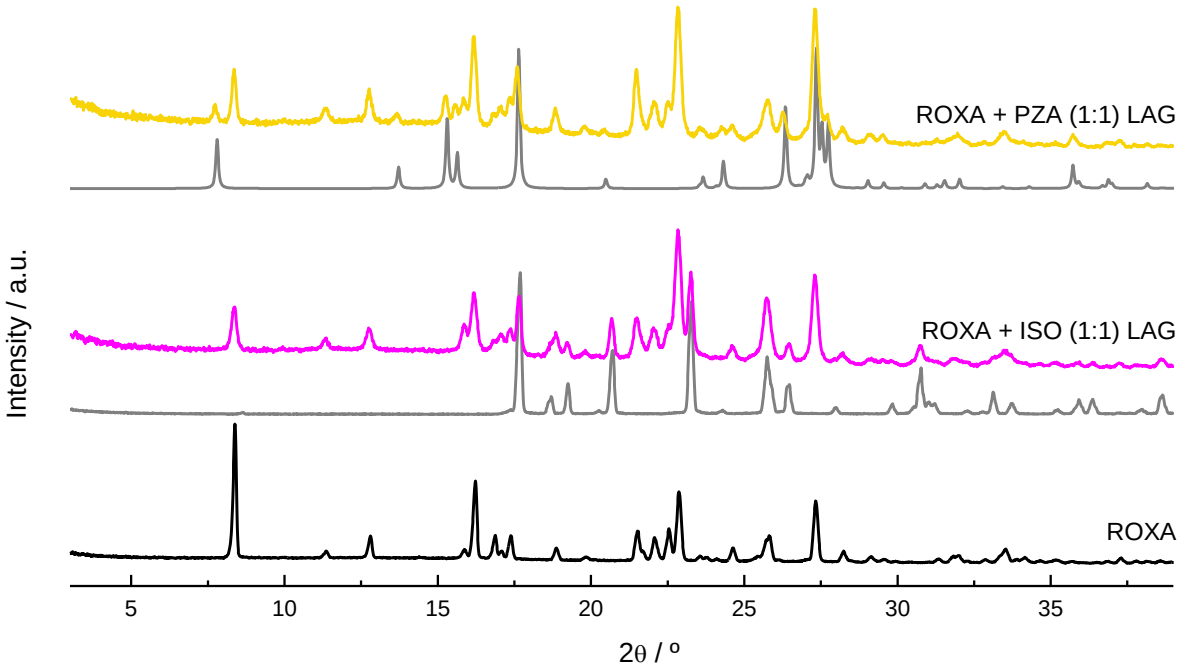

Figure 20 - XRPD diffractograms; roxadustat (black line), coformers (grey line) and respective solid mixtures

3.2.3. Roxadustat + Xanthines

Roxadustat + Caffeine

In this work, two xanthines (caffeine and theophylline) were studied in different molar ratios for binary mixtures with roxadustat. Mechanochemistry, namely LAG at 30 Hz for 30 min, was the method used for the synthesis. Caffeine was the only xanthine that could create a cocrystal, in an equimolar ratio, with the API under study. XRPD, DSC and FTIR-ATR were used as methods of characterization of this new multicomponent solid form.

The diffractograms of the mixture and of the pure compounds, roxadustat and caffeine, are shown in Figure 21. New reflections appear in the diffractogram of the mixture, particularly at 10.1°, 25.0° and 26.7°, indicating the presence of a new crystalline arrangement. In previous work carried out in our laboratory, equimolar mixtures of roxadustat with caffeine were investigated by mechanochemistry, but at 15 Hz for 30 minutes[92], and a cocrystal identified. The cocrystal obtained in the present work is the same, as it has an identical X-ray powder diffractogram.

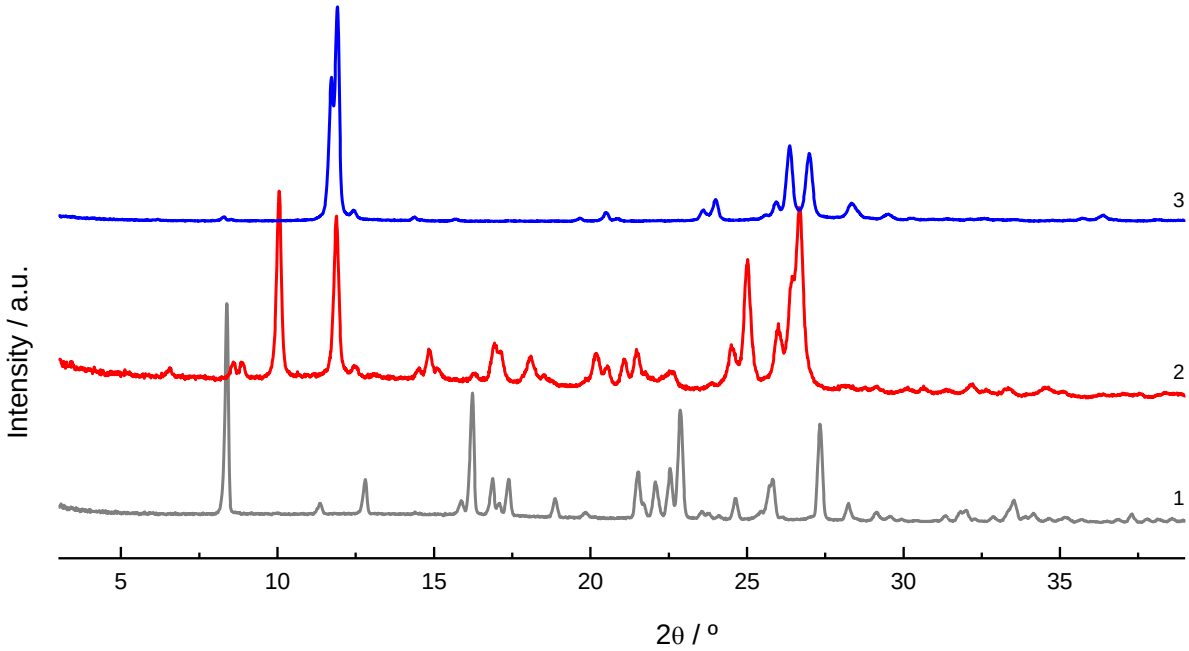

Figure 21 - XRPD diffractograms: 1. roxadustat; 2. roxadustat + caffeine (1:1) by LAG; 3. caffeine

The thermal behavior, analysed by DSC, is shown in Figure 22. The heating curve of the solid mixture, thermogram 2, manifests an endothermic event at T = 173.5 °C, corresponding to the fusion temperature.

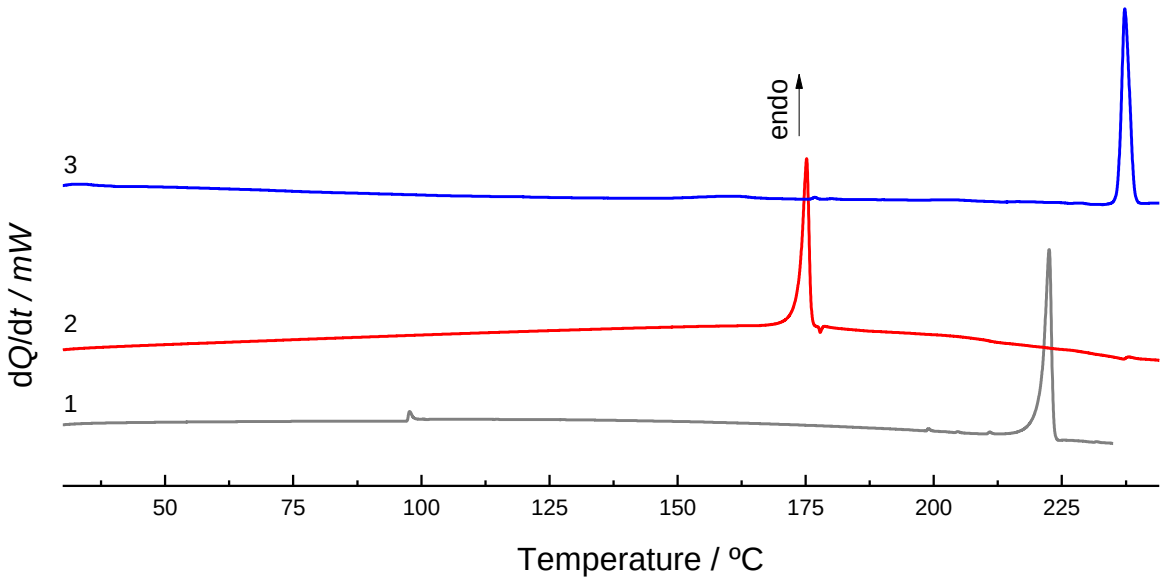

Figure 22 - DSC heating curves: 1. roxadustat; 2. roxadustat + caffeine (1:1) by LAG; 3. caffeine; β = 10 °C/min

The FTIR-ATR analysis, represented in Figure 23, shows the differences between the spectrum of the mixture, spectrum 2, and the spectra of the pure compounds, 1 and 3. The mixture shows a change in the 1695 - 1642 cm^{-1} band referring to the C=N elongation, which in the mixture is shifted to 1705 cm^{-1}.

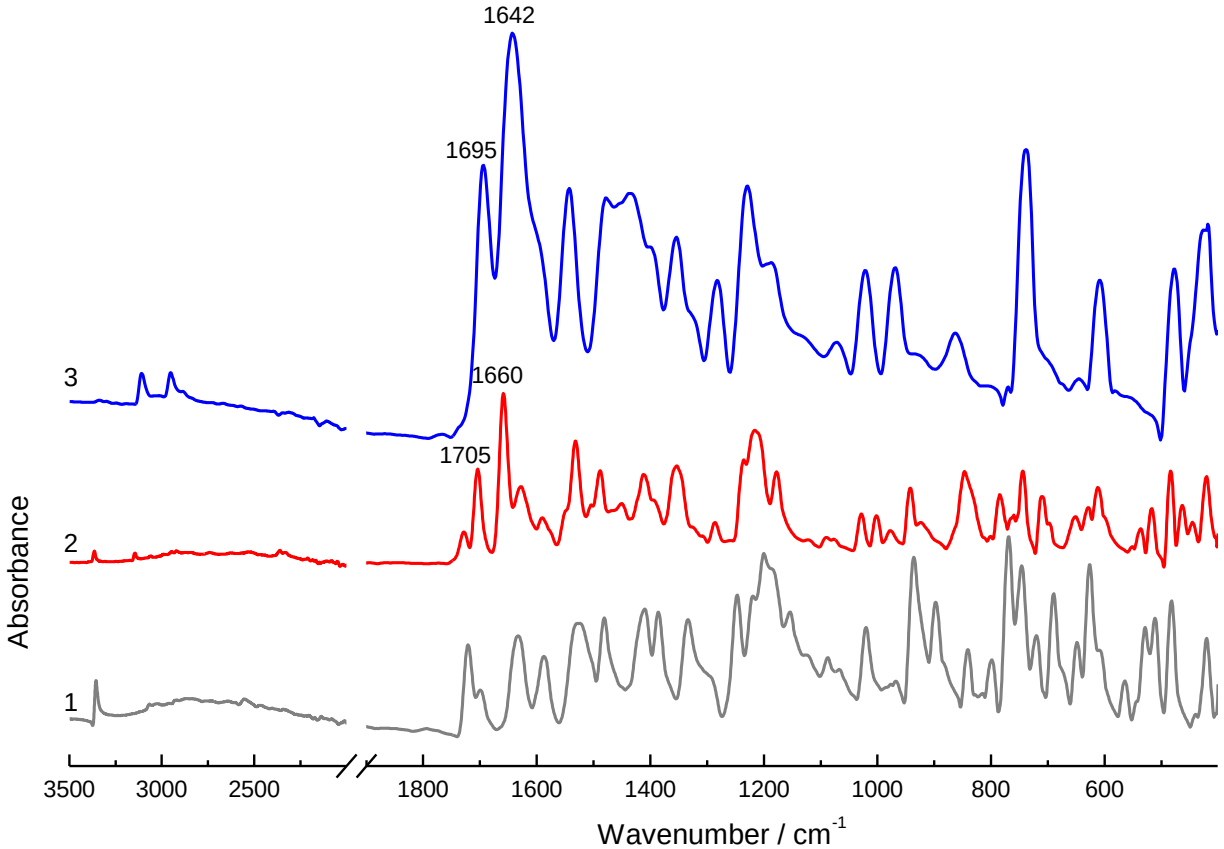

Figure 23 - FTIR spectra: 1. roxadustat; 2. roxadustat + caffeine (1:1) by LAG; 3. caffeine

Roxadustat + Theophylline

As already mentioned, among the xanthines studied, it was only possible to synthesize a cocrystal with caffeine. Theophylline was also studied in different molar rations with roxadustat by liquid assisted grinding at 30 Hz by 30 min. Despite the molecular similarity between the two xanthines, theophylline was not able to associate with roxadustat, as demonstrated in the diffractograms represented in Figure 24. Mixtures of molar rations of 2:1 and 1:2 of this binary system were also not able to produce a new solid form.

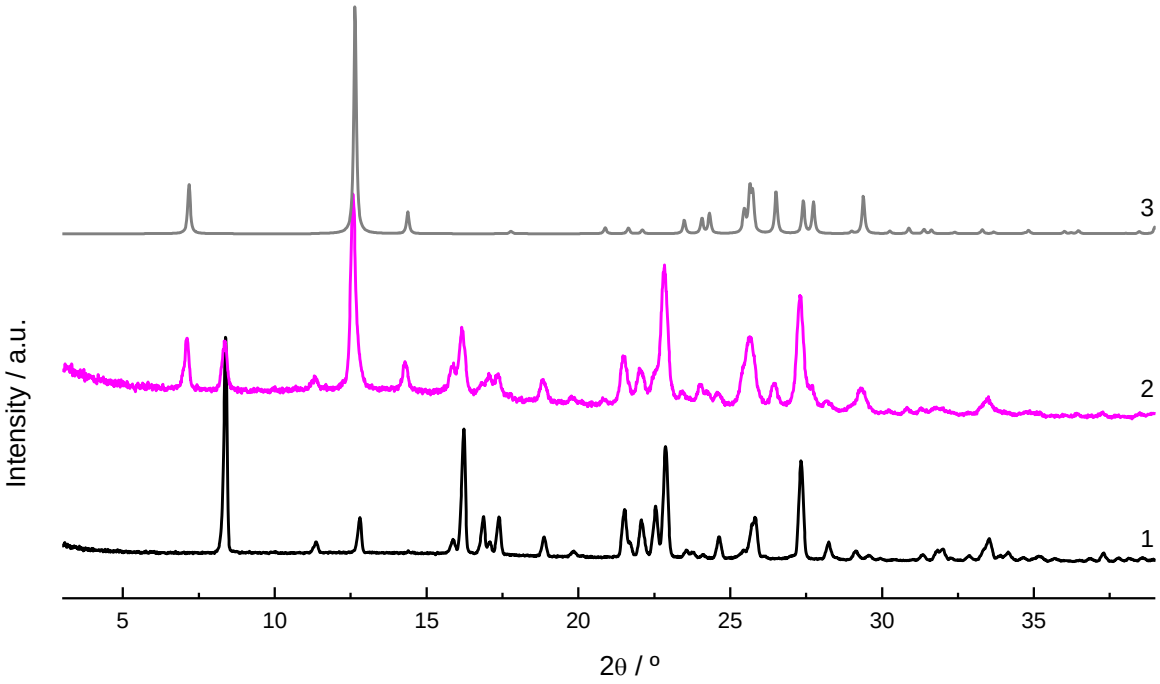

Figure 24 - XRPD diffractograms: 1. roxadustat; 2. roxadustat + theophylline (1:1) by LAG; 3. theophylline

3.2.4. Roxadustat + Amino acids

Roxadustat + L-histidine / Roxadustat + Cysteine / Roxadustat + Tryptophan

Several amino acids, such as, *L*-histidine, cysteine, and tryptophan were subjected to liquid assisted grinding at 30 Hz by 30 min in equimolar mixtures with roxadustat in order to try to synthesise new multicomponent solid forms. As shown in Figure 25, from the diffractograms obtained by XRPD, we conclude that these solid mixtures are only the sum of the roxadustat and the coformers used.

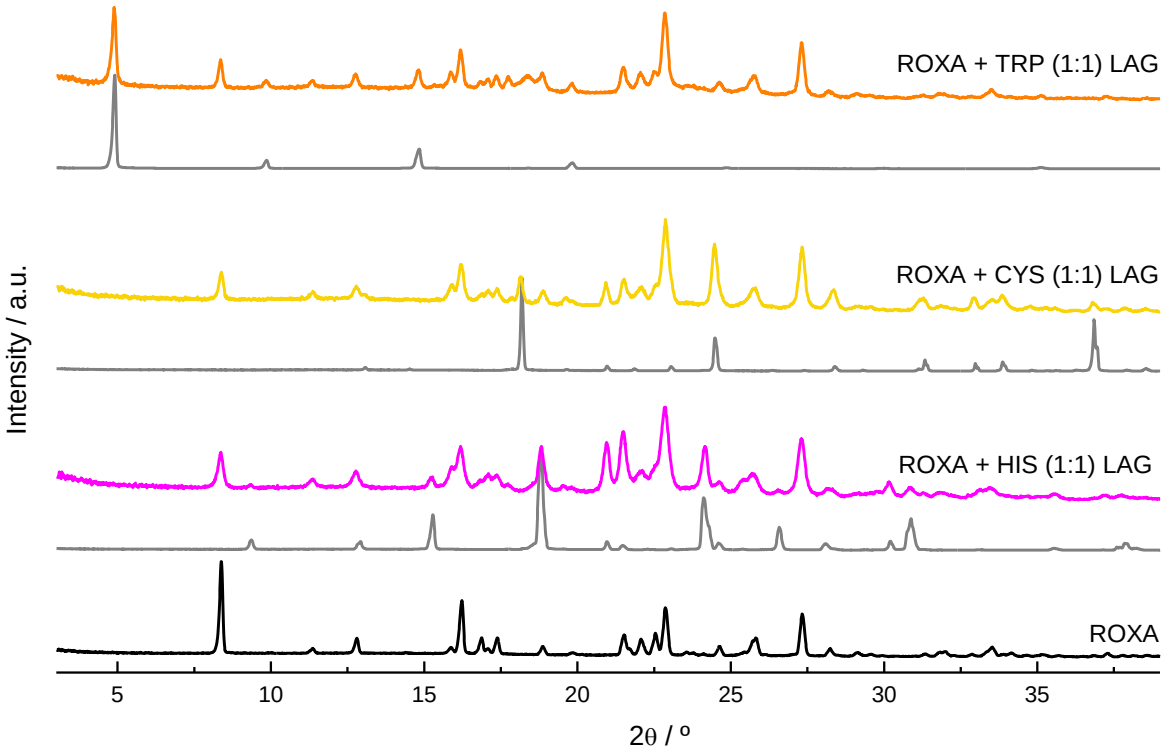

Figure 25 - XRPD diffractograms; roxadustat (black line), coformers (grey line) and respective solid mixtures

Roxadustat + Pyridoxine

In order to synthesize another coamorphous compound, pyridoxine was used in an equimolar ratio with roxadustat. This solid mixture was produced by neat grinding at 30 Hz during 30 min. The graph in Figure 26, compares the diffractograms of the solid mixture with the pure compounds, roxadustat and pyridoxine. Diffractogram 2 shows no reflections, which means that a coamorphous solid form was obtained from the mixture of roxadustat + pyridoxine (1:1). DSC and FTIR-ATR analyses were performed to further characterize this new multicomponent solid form.

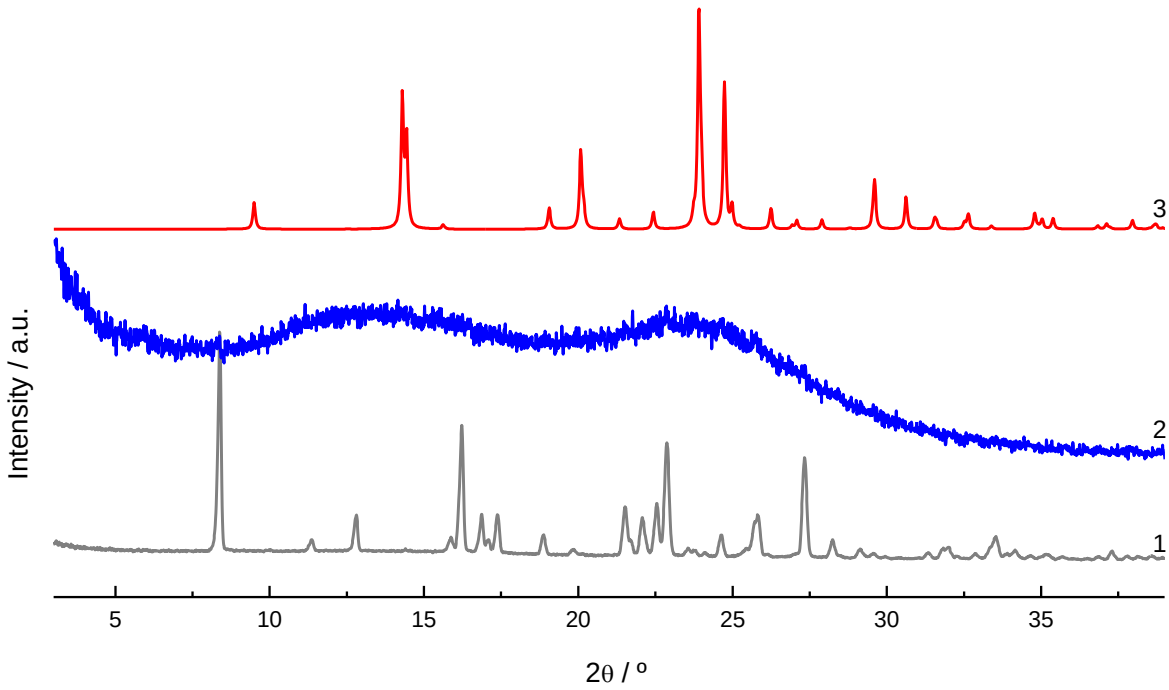

Figure 26 - XRPD diffractograms: 1. roxadustat; 2. roxadustat + pyridoxine (1:1) by NG; 3. pyridoxine

Figure 27 shows the thermal behaviour of the solid mixture with a *Tg* = 134.5 °C, however, as can be seen, it starts to degrade at *T* = 165 °C.

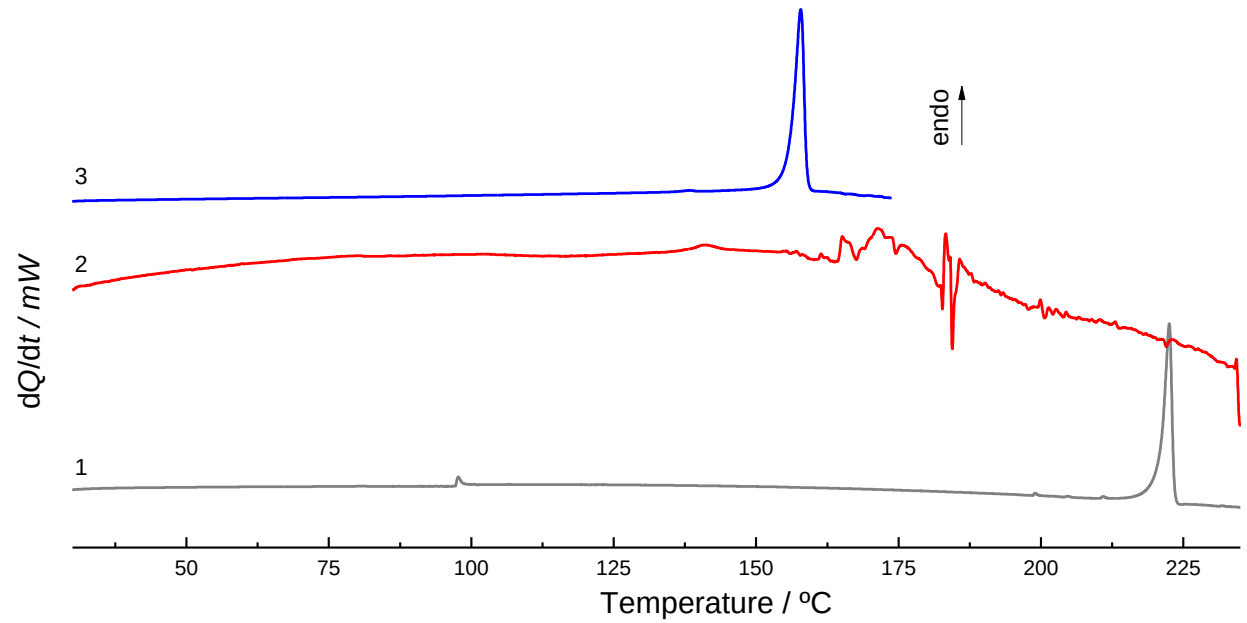

Figure 27 – DSC heating curves: 1. roxadustat; 2. roxadustat + pyridoxine (1:1) by NG; 3. pyridoxine; β = 10 °C/min

Figure 28 compares the infrared spectrum of the mixture with the pure compounds, roxadustat and pyridoxine. From its analysis, spectrum 2 shows a typical spectrum of a coamorphous compound, since its bands are broader compared to the spectra of the pure compounds.

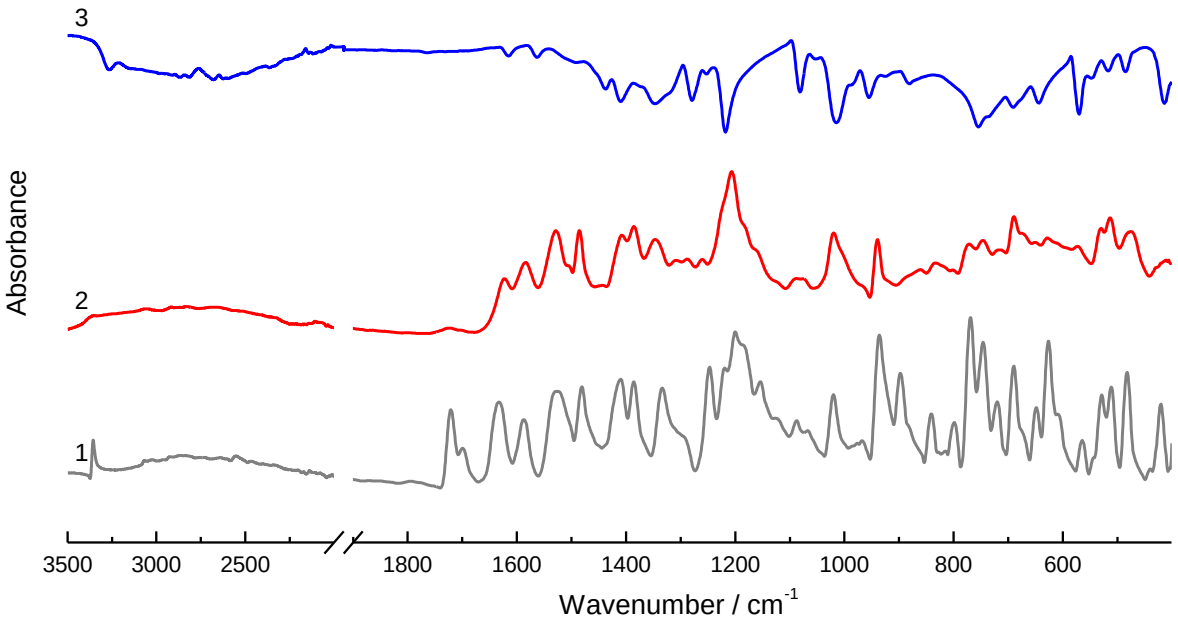

Figure 28 - FTIR spectra: 1. roxadustat; 2. roxadustat + pyridoxine (1:1) by NG; 3. pyridoxine

3.2.5. Roxadustat + Pyridine Derivatives and Pyrazine

Roxadustat + 1,2-Bis (4-pyridyl)ethane

Mixtures of roxadustat and 1,2-Bis (4-pyridyl)ethane were prepared by mechanochemistry with solvent addition (10 µl of ethanol) at 30 Hz for 30 min. Different molar ratios were prepared, however, it was in the ratio of 2:1 that a cocrystal was obtained. ROXA + BPA (2:1). The diffractograms shown in figure 29 compare the mixture with the pure compounds. Diffractogram 2 presents new peaks at 7.7°, 10.1° and 20.9°, suggesting the presence of a new crystalline arrangement.

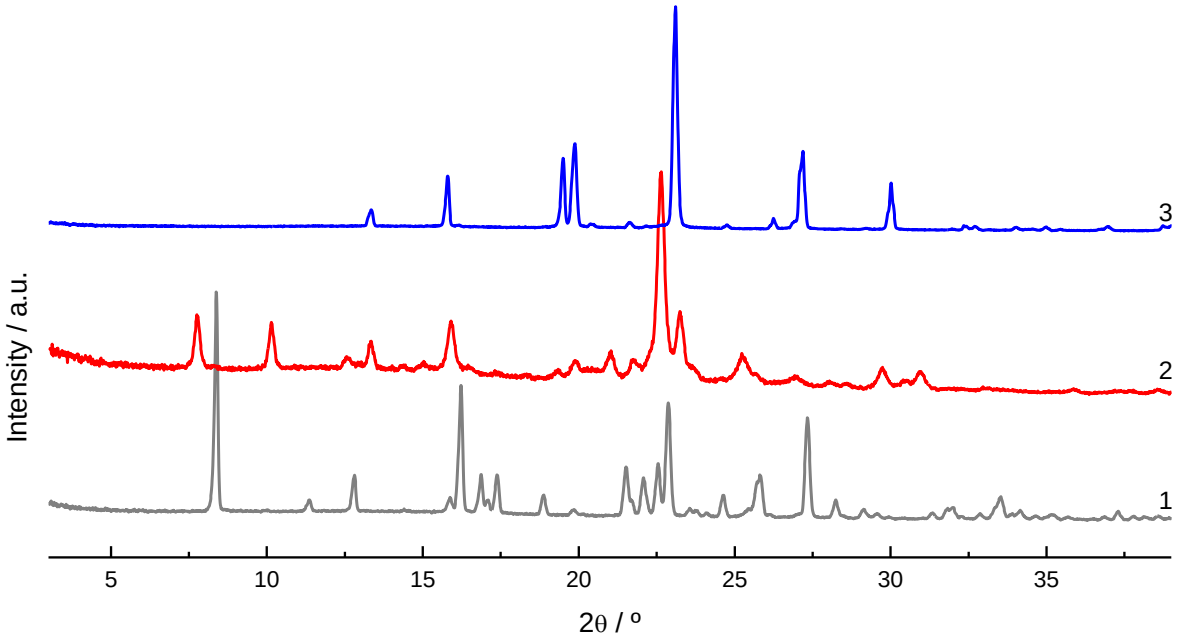

Figure 29 - XRPD diffractograms: 1. roxadustat; 2. roxadustat + 1,2 Bis (4-pyridyl)ethane (2:1) by LAG; 3. 1,2 Bis (4-pyridyl)ethane

Figure 30 represents the DSC heating curves of the mixture ROXA + BPA (2:1) and of the pure compounds. From its analysis, it is observed an endothermic event at T = 178.7 °C, the solid mixture fusion, which again is between the melting temperatures of pure compounds.

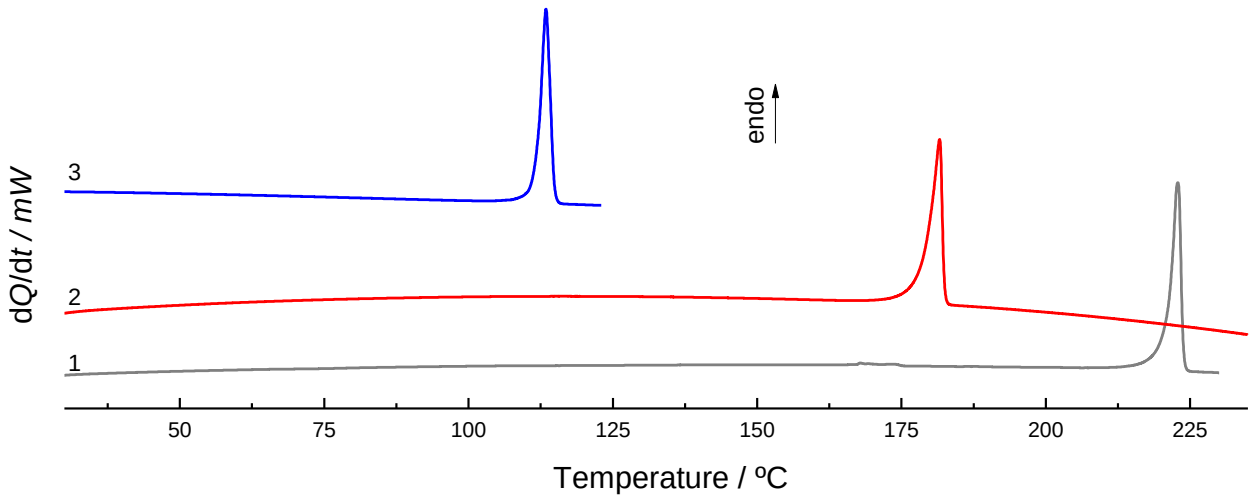

Figure 30 - DSC heating curves: 1. roxadustat; 2. roxadustat + 1,2 Bis (4-pyridyl)ethane (2:1) by LAG; 3. 1,2 Bis (4-pyridyl)ethane; β = 10 °C/min

The infrared spectrum of this new solid form is represented in Figure 31. The NH elongation, which appears at 3355 cm^{-1} in roxadustat, is displaced to 3405 cm^{-1} in the mixture spectrum. There is also the appearance of two bands centred at 2393 and 1913 cm^{-1} related to vibrational modes of the functional group OH when hydrogen bonded to an aromatic nitrogen atom. Analysis of the mixture´s spectrum also shows a change in the profile of the C=O group.

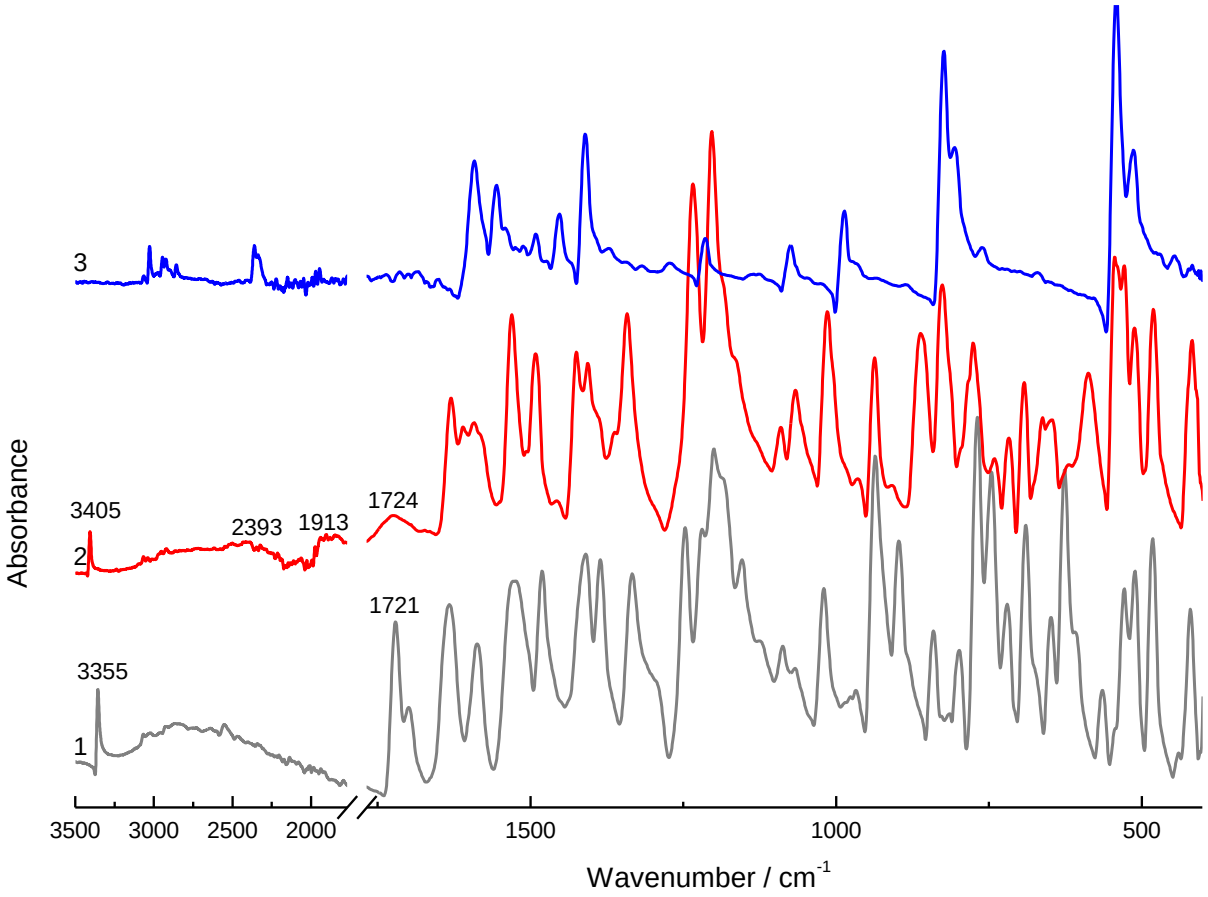

Figure 31 - FTIR spectra: 1. roxadustat; 2. roxadustat + 1,2 Bis (4-pyridyl)ethane (2:1) by LAG; 3. 1,2 Bis (4-pyridyl)ethane

Roxadustat + 4,4 Bipyridyl

Mixtures of roxadustat + 4,4 Bipyridyl were studied by mechanochemistry in different molar ration, with solvent addition. The new cocrystal represented in the following figures was obtained in a ratio of 2:1. The diffractogram of this new solid form, diffractogram 2, represented in Figure 32 shows new reflections when compared to the pure compounds, mainly at 7.5°, 10.0°, 15.1°, 18.2°, 20.2° and 24.4°, proposing the existence of a new crystalline arrangement.

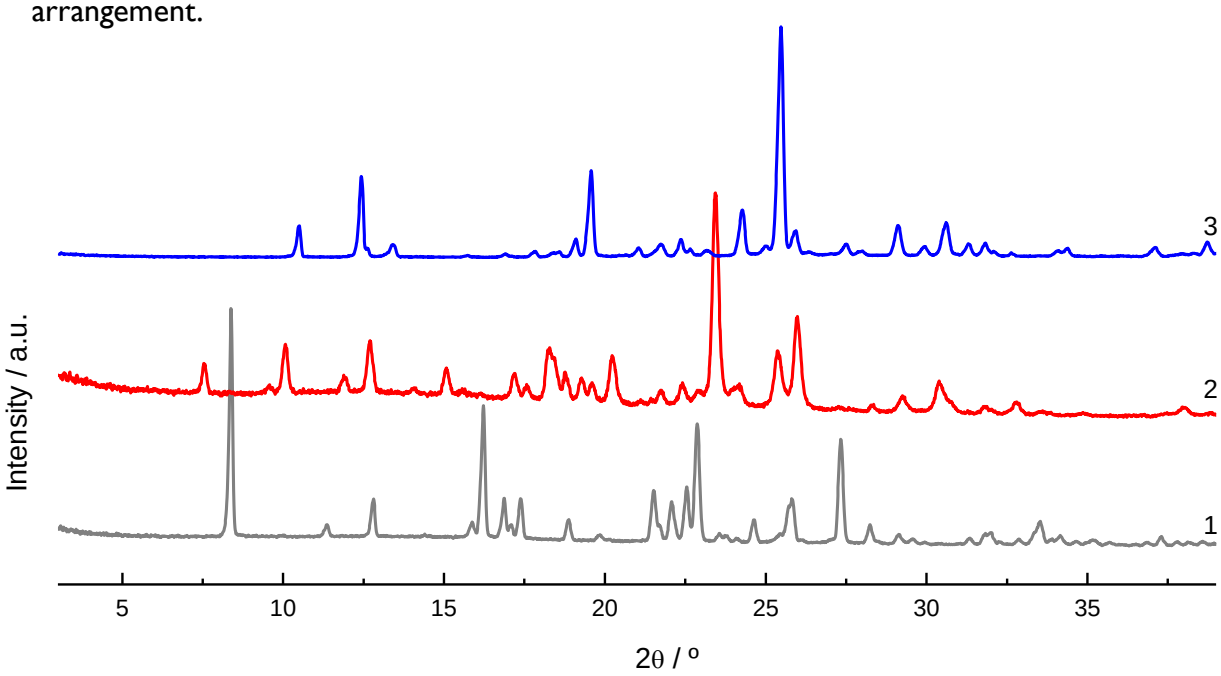

Figure 32 - XRPD diffractograms: 1. roxadustat; 2. roxadustat + 4,4 bipyridyl (2:1) by LAG; 3. 4,4 bipyridyl

The heating curve of this solid mixture, obtained by DSC, Figure 33, presents an endothermic event at a temperature value between the melting temperatures of the pure compounds, which is common in cocrystals. This endothermic event is a fusion of this mixture with a T = 164.8 °C.

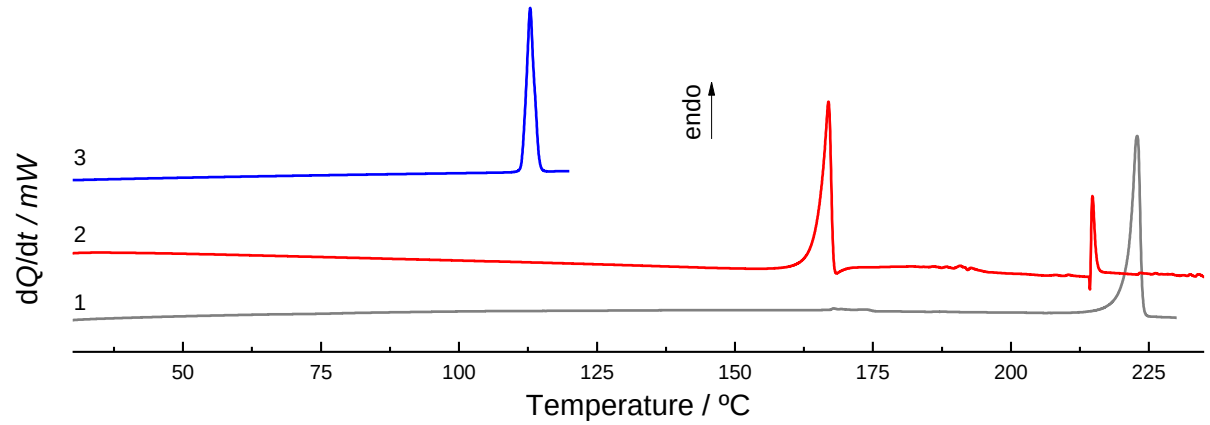

Figure 33 - DSC heating curves: 1. roxadustat; 2. roxadustat + 4,4 bipyridyl (2:1) by LAG; 3. 4,4 bipyridyl; β = 10 °C/min

FTIR-ATR spectrum represent is Figure 34, shows the differences between the mixture spectrum and the pure compounds, roxadustat and 4,4 bipyridyl. The roxadustat NH stretching band at 3355 cm^{-1}, is displaced to 3373 cm^{-1} in the mixture spectrum. As for roxadustat + 1,2 Bis (4-pyridyl)ethane (2:1), the heterosynthon COOH···$N_{aromatic}$ is identified from the new bands centred at 2331 and 1906 cm^{-1}. Analysis of the mixture´s spectrum shows a change in the profile of the C=O group.

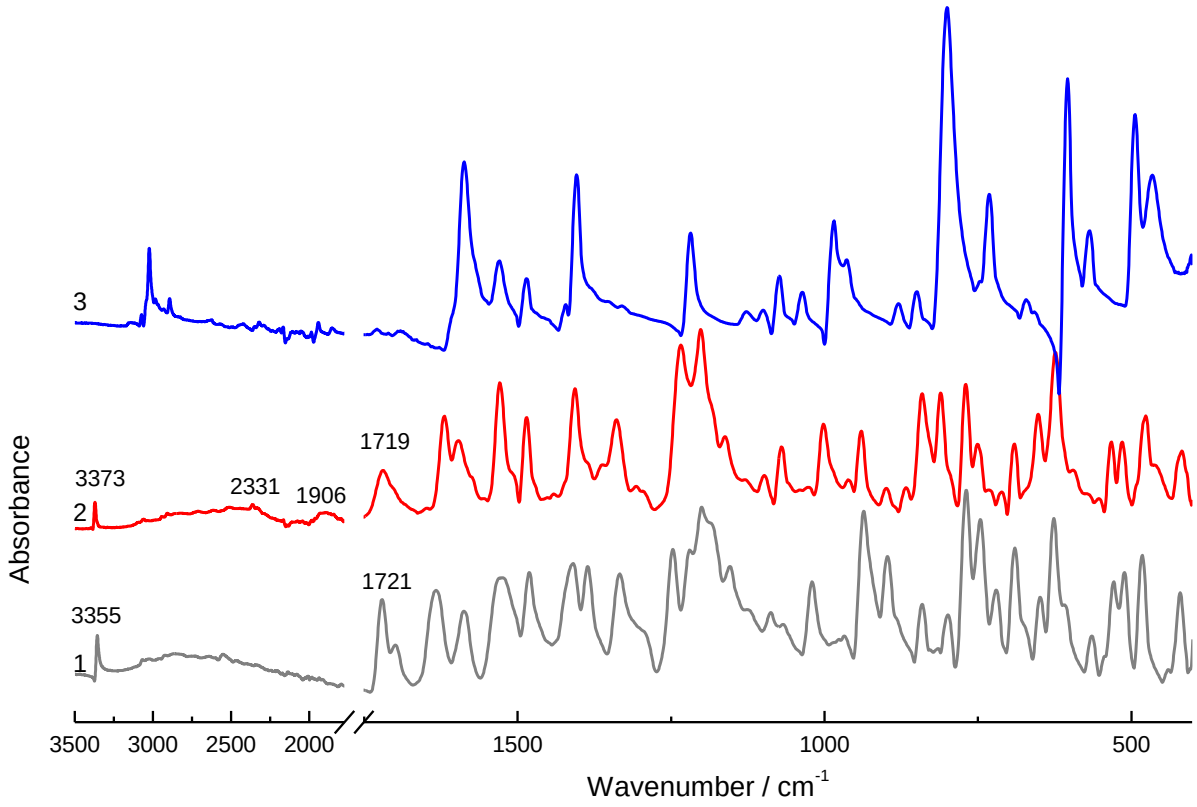

Figure 34 - FTIR spectra: 1. roxadustat; 2. roxadustat + 4,4 bipyridyl (2:1) by LAG; 3. 4,4 bipyridyl

Roxadustat + Pyrazine

The study of the roxadustat + pyrazine system began with the preparation of a 1:1 mixture by mechanochemistry, with solvent addition, at 30 Hz for 30 min. The solid form obtained was analysed by XRPD. The diffractogram of the mixture and the pure compounds, roxadustat and pyrazine, are shown in Figure 35. New reflections appear in the diffractogram of the mixture, namely at 9.90°, 11° and 13.9°, proposing the existence of a new crystalline arrangement. Reflections of starting materials are missing.

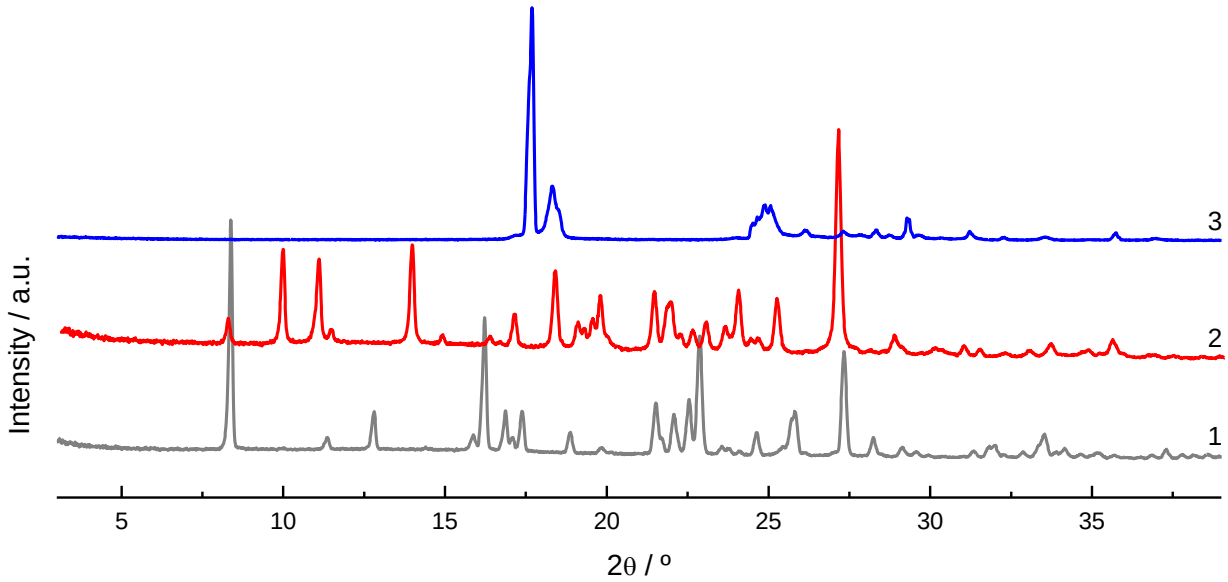

Figure 35 - XRPD diffractograms: 1. roxadustat; 2. roxadustat + pyrazine (1:1) by LAG; 3. pyrazine

New mixtures were prepared, with an excess of roxadustat or pyrazine compared to the equimolar mixture. Figure 36 shows the powder X-ray diffractograms of the pure compounds and of the mixtures in different proportions. In diffractogram 2, of the roxadustat+pyrazine (1:2) mixture, a reflection can be observed at 17.7°, - related to the excess of pyrazine, which is missing in the mixture (1:1). Diffractogram 4, referring to the mixture (2:1), is the same as the diffractogram of the equimolar mixture (diffractogram 3). Lastly, the diffractogram of the (3:1) mixture (diffractogram 5) shows several differences when compared to the diffractograms of the mixture (1:1) and (2:1), and the excess of roxadustat is clearly visible (for instance at 12.7° and 25.7°).

The difference between the diffractograms of the samples in various API:coformer proportions leads to the conclusion that a new cocrystal is formed, either in the proportion (2:1) or (1:1). Since the presence of an excess of roxadustat gives much pronounced signals than an excess of pyrazine - difference between the diffractograms of the mixtures (2:1) and (3:1) is bigger

than the difference between the mixtures (1:2) and (1:1) – the formation of a (2:1) cocrystal seems more likely.

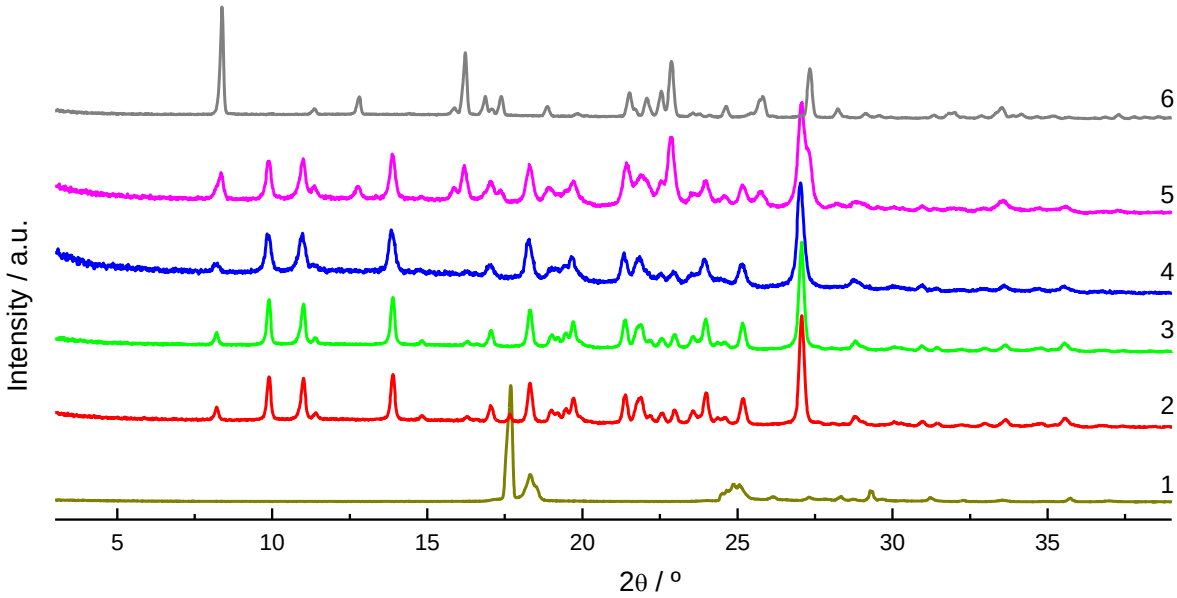

Figure 36 - XRPD diffractograms: 1. pyrazine; 2. roxadustat + pyrazine (1:2) by LAG; 3. roxadustat + pyrazine (1:1) by LAG; 4. roxadustat + pyrazine (2:1) by LAG; 5. roxadustat + pyrazine (3:1) by LAG; 6. roxadustat

The mixtures were also analysed by FTIR-ATR. Figure 37 compares the spectra of mixtures of (1:1) and (2:1) proportions with the pure compounds, roxadustat and pyrazine. The infrared spectrum of the mixture (2:1) is being compared here with that of mixture (1:1), since these are the proportions most likely to form a new crystalline arrangement with roxadustat. When comparing the spectrum of these two proportions, it is visible that both are the same, as was also observed in the powder X-ray diffraction analysis.

When comparing the mixtures with the pure compounds, the roxadustat NH stretching band, which appears at 3355 cm^{-1}, is displaced to 3387 cm^{-1} in the mixture spectrum and it also shows a change in the profile of the C=O group.

Efforts are being made, as for the other systems, to obtain single crystals in order to solve the crystal structure, which will be the definitive evidence of this cocrystal stoichiometry.

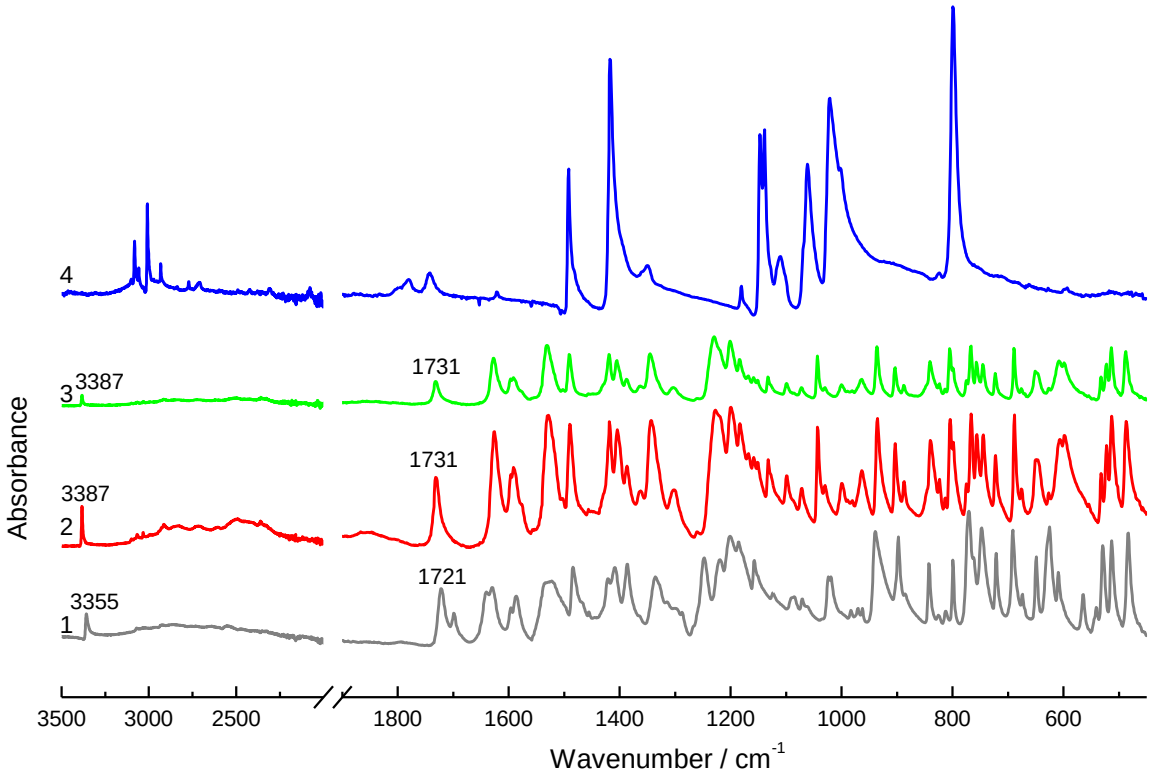

Figure 37 - FTIR spectra: 1. roxadustat; 2. roxadustat + pyrazine (1:1) by LAG; 3. roxadustat + pyrazine (2:1) by LAG; 4. pyrazine

3.3. Roxadustat solubility investigation

To study the equilibrium solubility of roxadustat, the saturation shake-flask method was used. Three systems were studied, including two cocrystals (ROXA+CAF, ROXA+NICO) and a coamorphous (ROXA+PYX) along with the pure compound.

Firstly, a calibration curve was made using roxadustat standard solutions of different concentrations, analysed by UV-Visible spectroscopy, measuring the respective absorbance at a wavelength of 360 nm, as shown in Figure 38 (A). This wavelength was suggested for quantification of roxadustat in alkaline medium - the fully deprotonated specimen.[91] Spectra for solutions of different concentration are illustrated in Figure 38 (B).

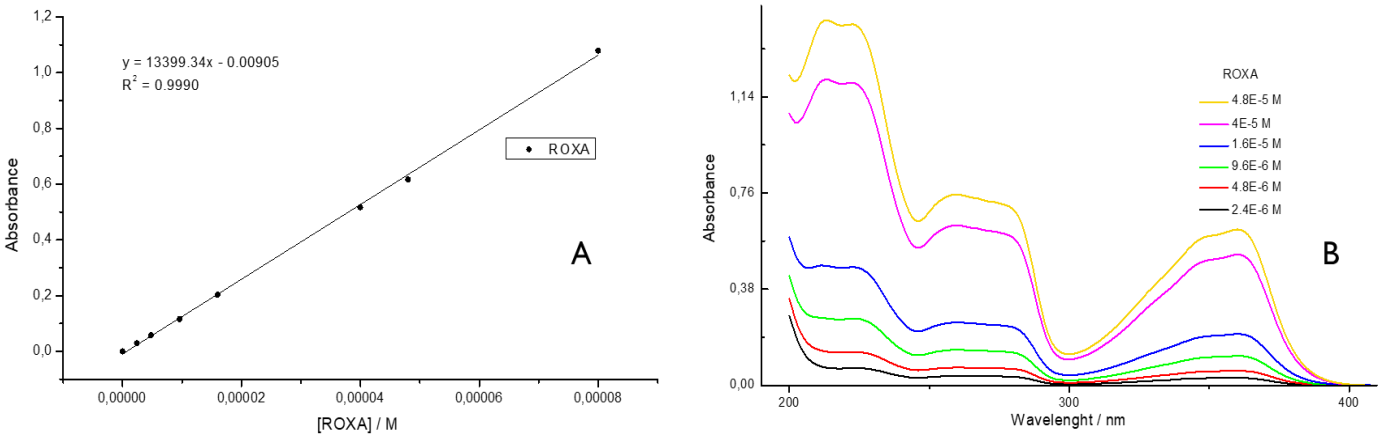

Figure 38 - Calibration curve of roxadustat (absorbance values registered at λ = 360 nm) **(A)** and UV-Vis spectra of solutions of different roxadustat concentrations **(B)**.

Once the calibration curve and its equation had been obtained, the solutions from the saturation shake-flask experiments were analysed. The absorbance values were recorded at λ = 360 nm by UV-Vis spectrometry and then the concentration of each sample was calculated from the calibration curve equation ($y = 13399.34x - 0.00905$). Finally, their mean and standard deviation were calculated both for equilibrium with roxadustat pure samples and with the solid mixtures, as shown in the following table, Table 2.

Table 2 - Mean concentrations of roxadustat and standard deviation of the different samples

Solid mixture	Mean / M	Standard Deviation / M
ROXA	1.41E-05	2.23E-06
ROXA + CAF	1.53E-05	2.54E-07
ROXA + NICO	1.54E-05	2.72E-06
ROXA + PYX	1.73E-04	9.32E-06

From the analysis of the Table 2, comparing the mean of roxadustat solubility when using the two cocrystals with that of the samples of pure roxadustat, we can see they are similar, which may mean that there has been complete dissolution of the coformers and reprecipitation of the API. These results show that the solubility of the active substance when combined in these cocrystals (with caffeine and nicotinamide) does not increase. On the other hand, the combination of roxadustat + pyridoxine (1:1) showed a significant increase in the solubility value when compared to pure roxadustat .

The samples under study were also analysed by XRPD in order to identify whether or not they had undergone any change in their solid forms after the solubility study by saturation shake- flask method. Starting with the pure roxadustat sample, it can be concluded, from the analysis of the diffractograms in Figure 39, that the initial roxadustat sample did not undergo any changes in its solid form after the investigation carried out.

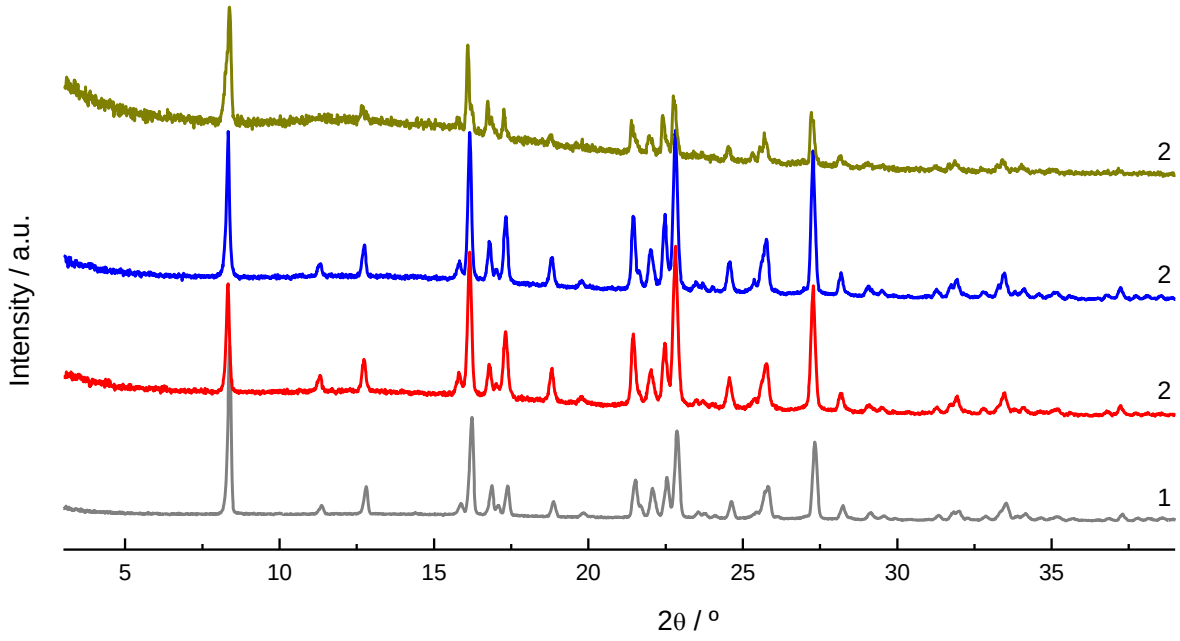

Figure 39 - XRPD diffractograms: 1. starting sample of roxadustat; 2. roxadustat samples after saturation shake-flask method investigation

The following graphics (Figures 40 and 41) represent the XRPD analysis for the two cocrystals studied. Both cocrystals (ROXA + CAF and ROXA + NICO) used in this research showed changes in their solid form when subjected to XRPD analysis after studying their solubility using the method mentioned above. Analysis of these diffractograms shows that the diffractogram obtained for all the samples, after solubility essays, is the same as the diffractogram of the roxadustat sample. This confirms the hypothesis claimed above and justify why the solubility values are the identical to that of pure roxadustat.

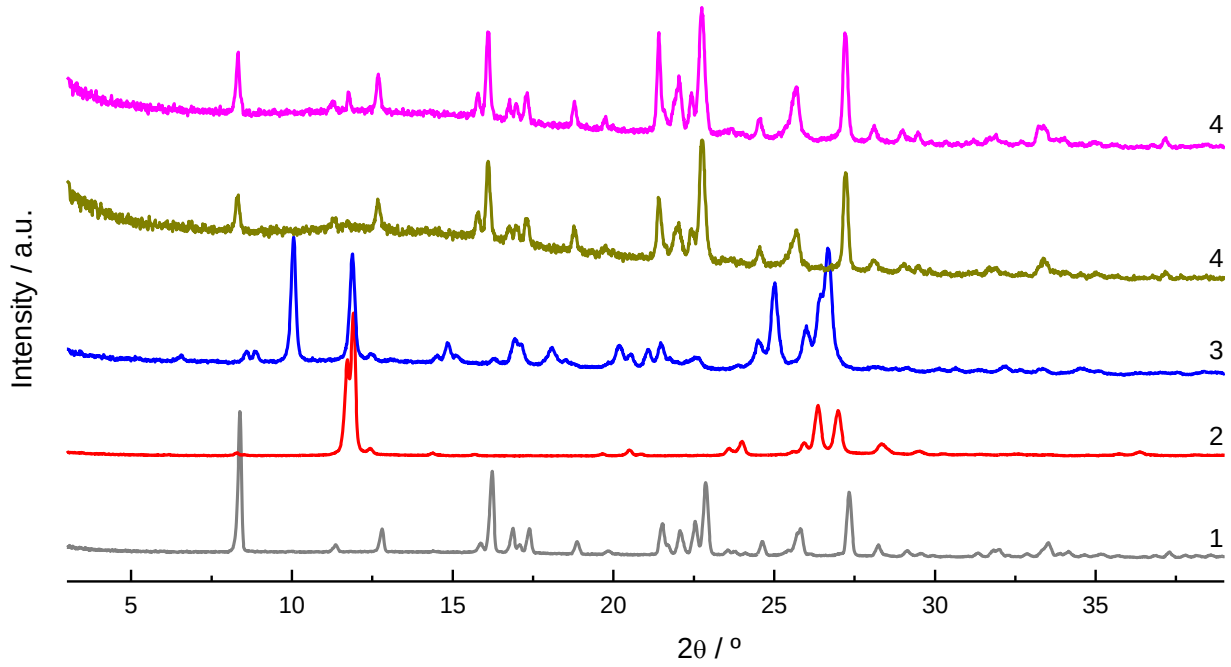

Figure 40 - XRPD diffractograms: 1. starting sample of roxadustat; 2. caffeine; 3. roxadustat + caffeine (1:1) by LAG; 4. ROXA + CAF (1:1) samples after saturation shake-flash method investigation

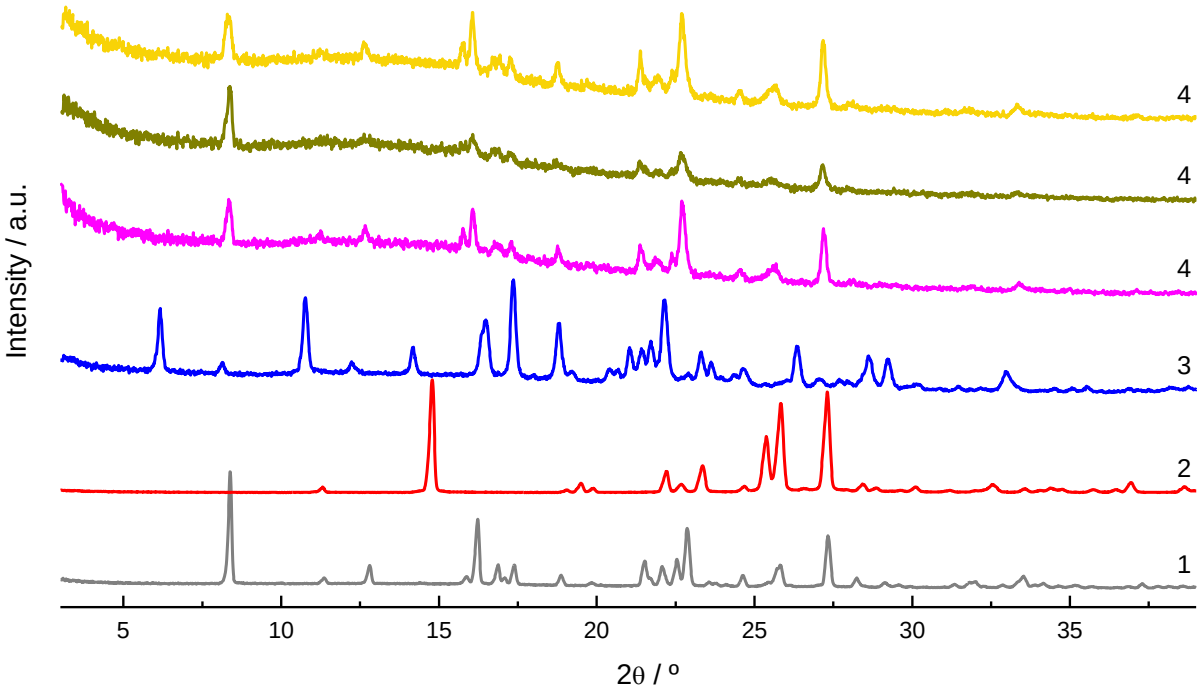

Figure 41 - XRPD diffractograms: 1. starting sample of roxadustat; 2. nicotinamide; 3. roxadustat + nicotinamide (1:1) by LAG; 4. ROXA + NICO (1:1) samples after saturation shake-flash method investigation

The solubility of roxadustat from the roxadustat + pyridoxine (1:1) coamorphous was also studied in this investigation and the remaining solid analysed by XRPD to verify whether the solid form had changed or not. These results are shown in Figure 42.

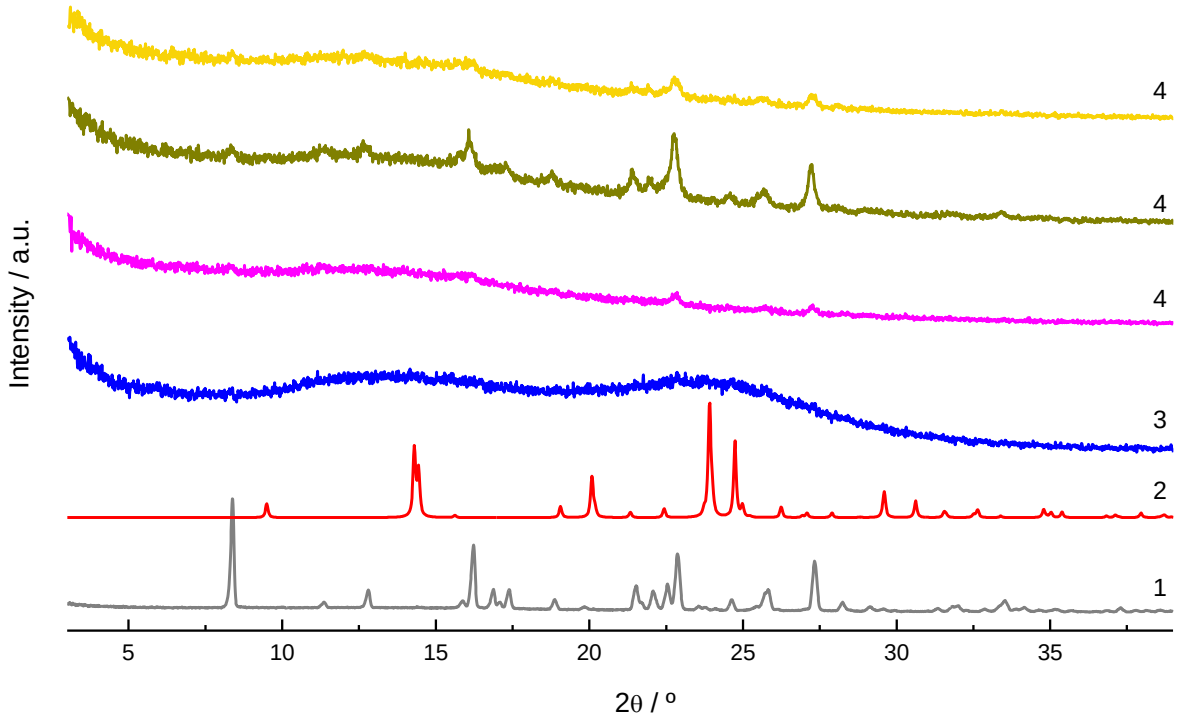

Figure 42 - XRPD diffractograms: 1. starting sample of roxadustat; 2. pyridoxine; 3. roxadustat + pyridoxine (1:1) by NG; 4. ROXA + PYX (1:1) samples after saturation shake-flash method investigation

When analysing the diffractograms of the coamorphous samples, it can be seen that they remain essentially amorphous, even after studying their solubility using the saturation shake-flask method.

The ROXA + PYX (1:1) system remained amorphous after its solubility study which justifies the increase in roxadustat solubility observed.

4. CONCLUSION

Roxadustat solid behaviour has proved to be a complex, yet interesting object of study. In this work, it was possible to investigate the ability of this active pharmaceutical ingredient, used in the treatment of anemia associated with CKD, to form new solid forms with different coformers in order to improve its efficacy and safety. The solubility of this compound was also studied.

Mechanochemistry (neat and liquid assisted grinding) was used as the technique for cocrystal, amorphous and coamorphous synthesis. The samples obtained were characterized by calorimetric methods (DSC) and spectroscopy methods (FTIR-ATR and XRPD).

The amorphization of roxadustat was possible by neat grinding at 30 Hz for 60 min only. Liquid assisted grinding (10 µl of ethanol) at 30 Hz for 30 min resulted in the synthesis of new cocrystals with hydrogen bond acceptor coformers such as 1,2-bis(4-pyridyl)ethane (2:1), pyrazine (2:1), 4,4 bipyridyl (2:1) and caffeine (1:1). No association occurred with theophylline; the other xanthine investigated. Cocrystals were also obtained by LAG with benzamide (1:1) and nicotinamide (1:1), but not with pyrazinamide, which is more complex concerning functional groups.

Two coamorphous phases, roxadustat:folic acid (1:1) and roxadustat:pyridoxine (1:1), were synthesized by neat grinding at 30 Hz for 30 min.

The other coformers used did not shown any association with roxadustat.

Solubility determination was carried out by the saturation shake-flask method for two cocrystals and a coamorphous mixture obtained by mechanochemistry, which were chosen due to their pharmaceutical properties: ROXA + NICO and ROXA + CAF (1:1) cocrystals and ROXA + PYX (1:1) coamorphous system. It was concluded, from XRPD analysis, that in the essays with the cocrystals, roxadustat reprecipitated from the solution and the coformers dissolve completely. The solubility values obtained are, therefore, identical to that of pure roxadustat. On the other hand, the coamorphous ROXA:PYX (1:1) system remained amorphous, even after the study by saturation shake-flask method and a higher roxadustat solubility was obtained relatively to the pure crystalline drug.

In short, this investigation has provided useful information on the behavior of roxadustat in the solid state, with new cocrystals and amorphous phases identified. It also contributed to the investigation of the solubility of this active pharmaceutical ingredient, alone and in multicomponent systems.

For future projects, it would be interesting to continue the investigation of multicomponent systems of this API with different coformers, as well as study their solubility and also dissolution rate, since there is a great lack of data in literature on this subject for this drug.

References

(1) Aitipamula, S.; Banerjee, R.; Bansal, A. K.; Biradha, K.; Cheney, M. L.; Choudhury, A. R.; Desiraju, G. R.; Dikundwar, A. G.; Dubey, R.; Duggirala, N.; Ghogale, P. P.; Ghosh, S.; Goswami, P. K.; Goud, N. R.; Jetti, R. R. K. R.; Karpinski, P.; Kaushik, P.; Kumar, D.; Kumar, V.; Moulton, B.; Mukherjee, A.; Mukherjee, G.; Myerson, A.; Puri, V.; Ramanan, A.; Rajamannar, T.; Reddy, C. M.; Rodriguez-Hornedo, N.; Rogers, R. D.; Row, T. N. G.; Sanphui, P.; Shan, N.; Shete, G.; Singh, A.; Sun, C. C.; Swift, J. A.; Thaimattam, R.; Thakur, T. S.; Thaper, R. K.; Thomas, S.; Tothadi, S.; Vangala, V. R.; Variankaval, N.; Vishweshwar, P.; Weyna, D. R.; Zaworotko, M. J. Polymorphs, Salts, and Cocrystals: What's in a Name? Cryst. Growth Des. **2012**, *12*, 2147−2152. https://doi.org/10.1021/cg3002948.

(2) Raza, K.; Kumar, P.; Ratan, S.; Malik, R.; Arora, S. Polymorphism: The Phenomenon Affecting the Performance of Drugs. *SOJ Pharmacy & Pharmaceutical Sciences* **2014**, *1* (2).

(3) Kawakami, K. Reversibility of Enantiotropically Related Polymorphic Transformations from a Practical Viewpoint: Thermal Analysis of Kinetically Reversible/Irreversible Polymorphic Transformations. J. Pharm. Sci. **2007**, *96* (5), 982–989. https://doi.org/10.1002/jps.20748.

(4) Burger, A.; Ramberger, R. On the Polymorphism of Pharmaceuticals and Other Molecular Crystals. I. *Mikrochim Acta* **1979**, *72* (3), 259–271. https://doi.org/10.1007/BF01197379.

(5) Lee, A. Y.; Erdemir, D.; Myerson, A. S. Crystal Polymorphism in Chemical Process Development. *Annu Rev Chem Biomol Eng* **2011**, *2*, 259–280. https://doi.org/10.1146/annurev-chembioeng-061010-114224.

(6) Cerreia Vioglio, P.; Chierotti, M. R.; Gobetto, R. Pharmaceutical Aspects of Salt and Cocrystal Forms of APIs and Characterization Challenges. *Adv Drug Deliv Rev* **2017**, *117*, 86–110. https://doi.org/10.1016/j.addr.2017.07.001.

(7) Haleblian, J.; McCrone, W. Pharmaceutical Applications of Polymorphism. J. Pharm. Sci. **1969**, *58* (8), 911–929. https://doi.org/10.1002/jps.2600580802.

(8) Guo, M.; Sun, X.; Chen, J.; Cai, T. Pharmaceutical Cocrystals: A Review of Preparations, Physicochemical Properties and Applications. *Acta Pharmaceutica Sinica B* **2021**, *11* (8), 2537–2564. https://doi.org/10.1016/j.apsb.2021.03.030.

(9) Koranne, S.; Krzyzaniak, J. F.; Luthra, S.; Arora, K. K.; Suryanarayanan, R. Role of Coformer and Excipient Properties on the Solid-State Stability of Theophylline Cocrystals. Cryst. Growth Des. **2019**, *19* (2), 868–875. https://doi.org/10.1021/acs.cgd.8b01430.

(10) Qiao, N.; Li, M.; Schlindwein, W.; Malek, N.; Davies, A.; Trappitt, G. Pharmaceutical Cocrystals: An Overview. *Int J Pharm* **2011**, *419* (1–2), 1–11. https://doi.org/10.1016/j.ijpharm.2011.07.037.

(11) Yadav, A. V.; Shete, A. S.; Dabke, A. P.; Kulkarni, P. V.; Sakhare, S. S. Co-Crystals: A Novel Approach to Modify Physicochemical Properties of Active Pharmaceutical Ingredients. *Indian J Pharm Sci* **2009**, *71* (4), 359–370. https://doi.org/10.4103/0250-474X.57283.

(12) Perlovich, G. L. Thermodynamic Characteristics of Cocrystal Formation and Melting Points for Rational Design of Pharmaceutical Two-Component Systems. *CrystEngComm* **2015**, *17* (37), 7019–7028. https://doi.org/10.1039/C5CE00992H.

(13) Kumar Bandaru, R.; Rout, S. R.; Kenguva, G.; Gorain, B.; Alhakamy, N. A.; Kesharwani, P.; Dandela, R. Recent Advances in Pharmaceutical Cocrystals: From Bench to Market. *Front Pharmacol* **2021**, *12*, 780582. https://doi.org/10.3389/fphar.2021.780582.

(14) Fukte, S. R.; Wagh, M. P.; Rawat, S. COFORMER SELECTION: AN IMPORTANT TOOL IN COCRYSTAL FORMATION. Int. J. Pharm. Sci. **2014**, 9–14.

(15) Yuliandra, Y.; Zaini, E.; Syofyan, S.; Pratiwi, W.; Putri, L. N.; Pratiwi, Y. S.; Arifin, H. Cocrystal of Ibuprofen–Nicotinamide: Solid-State Characterization and In Vivo Analgesic Activity Evaluation. *Sci Pharm* **2018**, *86* (2), 23. https://doi.org/10.3390/scipharm86020023.

(16) Wang, X.; Du, S.; Zhang, R.; Jia, X.; Yang, T.; Zhang, X. Drug-Drug Cocrystals: Opportunities and Challenges. *Asian J Pharm Sci* **2021**, *16* (3), 307–317. https://doi.org/10.1016/j.ajps.2020.06.004.

(17) Karimi-Jafari, M.; Padrela, L.; Walker, G. M.; Croker, D. M. Creating Cocrystals: A Review of Pharmaceutical Cocrystal Preparation Routes and Applications. *Cryst. Growth Des.* **2018**, *18* (10), 6370–6387. https://doi.org/10.1021/acs.cgd.8b00933.

(18) Hossain Mithu, M. S.; Ross, S. A.; Hurt, A. P.; Douroumis, D. Effect of Mechanochemical Grinding Conditions on the Formation of Pharmaceutical Cocrystals and Co-Amorphous Solid Forms of Ketoconazole – Dicarboxylic Acid.J Drug Deliv Sci Technol **2021**, *63*, 102508. https://doi.org/10.1016/j.jddst.2021.102508.

(19) Healy, A. M.; Worku, Z. A.; Kumar, D.; Madi, A. M. Pharmaceutical Solvates, Hydrates and Amorphous Forms: A Special Emphasis on Cocrystals. *Adv Drug Deliv Rev* **2017**, *117*, 25–46. https://doi.org/10.1016/j.addr.2017.03.002.

(20) Chadha, R.; Kuhad, A.; Arora, P.; Kishor, S. Characterisation and Evaluation of Pharmaceutical Solvates of Atorvastatin Calcium by Thermoanalytical and Spectroscopic Studies. *Chem. Cent. J.* **2012**, *6* (1), 114. https://doi.org/10.1186/1752-153X-6-114.

(21) Mattia, E.; Otto, S. Supramolecular Systems Chemistry. *Nat Nanotechnol* **2015**, *10* (2), 111–119. https://doi.org/10.1038/nnano.2014.337.

(22) Vippagunta, S. R.; Brittain, H. G.; Grant, D. J. Crystalline Solids. *Adv Drug Deliv Rev* **2001**, *48* (1), 3–26. https://doi.org/10.1016/s0169-409x(01)00097-7.

(23) Baghel, S.; Cathcart, H.; O'Reilly, N. J. Polymeric Amorphous Solid Dispersions: A Review of Amorphization, Crystallization, Stabilization, Solid-State Characterization, and Aqueous Solubilization of Biopharmaceutical Classification System Class II Drugs. *J Pharm Sci* **2016**, *105* (9), 2527–2544. https://doi.org/10.1016/j.xphs.2015.10.008.

(24) Gurunath, S.; Pradeep Kumar, S.; Basavaraj, N. K.; Patil, P. A. Amorphous Solid Dispersion Method for Improving Oral Bioavailability of Poorly Water-Soluble Drugs. *J. Pharm. Res.* **2013**, *6* (4), 476–480. https://doi.org/10.1016/j.jopr.2013.04.008.

(25) Qi, S.; McAuley, W. J.; Yang, Z.; Tipduangta, P. Physical Stabilization of Low-Molecular-Weight Amorphous Drugs in the Solid State: A Material Science Approach. *Ther Deliv* **2014**, *5* (7), 817–841. https://doi.org/10.4155/tde.14.39.

(26) Murdande, S. B.; Pikal, M. J.; Shanker, R. M.; Bogner, R. H. Solubility Advantage of Amorphous Pharmaceuticals: I. A Thermodynamic Analysis. *J Pharm Sci* **2010**, *99* (3), 1254–1264. https://doi.org/10.1002/jps.21903.

(27) Hancock, B. C.; Zografi, G. Characteristics and Significance of the Amorphous State in Pharmaceutical Systems. *J Pharm Sci* **1997**, *86* (1), 1–12. https://doi.org/10.1021/js9601896.

(28) Debenedetti, P. G.; Stillinger, F. H. Supercooled Liquids and the Glass Transition. *Nature* **2001**, *410* (6825), 259–267. https://doi.org/10.1038/35065704.

(29) Löbmann, K.; Laitinen, R.; Grohganz, H.; Gordon, K. C.; Strachan, C.; Rades, T. Coamorphous Drug Systems: Enhanced Physical Stability and Dissolution Rate of Indomethacin and Naproxen. *Mol Pharm* **2011**, *8* (5), 1919–1928. https://doi.org/10.1021/mp2002973.

(30) Han, J.; Wei, Y.; Lu, Y.; Wang, R.; Zhang, J.; Gao, Y.; Qian, S. Co-Amorphous Systems for the Delivery of Poorly Water-Soluble Drugs: Recent Advances and an Update. *Expert Opin Drug Deliv* **2020**, *17* (10), 1411–1435. https://doi.org/10.1080/17425247.2020.1796631.

(31) Shi, Q.; Moinuddin, S. M.; Cai, T. Advances in Coamorphous Drug Delivery Systems. *Acta Pharm Sin B* **2019**, *9* (1), 19–35. https://doi.org/10.1016/j.apsb.2018.08.002.

(32) Karagianni, A.; Kachrimanis, K.; Nikolakakis, I. Co-Amorphous Solid Dispersions for Solubility and Absorption Improvement of Drugs: Composition, Preparation, Characterization and Formulations for Oral Delivery. *Pharmaceutics* **2018**, *10* (3), 98. https://doi.org/10.3390/pharmaceutics10030098.

(33) Liu, J.; Grohganz, H.; Löbmann, K.; Rades, T.; Hempel, N.-J. Co-Amorphous Drug Formulations in Numbers: Recent Advances in Co-Amorphous Drug Formulations with Focus on Co-Formability, Molar Ratio, Preparation Methods, Physical Stability, In Vitro and In Vivo Performance, and New Formulation Strategies. *Pharmaceutics* **2021**, *13* (3), 389. https://doi.org/10.3390/pharmaceutics13030389.

(34) Dengale, S. J.; Grohganz, H.; Rades, T.; Löbmann, K. Recent Advances in Co-Amorphous Drug Formulations. *Adv. Drug Deliv. Rev.* **2016**, *100*, 116–125. https://doi.org/10.1016/j.addr.2015.12.009.

(35) Su, M.; Xia, Y.; Shen, Y.; Heng, W.; Wei, Y.; Zhang, L.; Gao, Y.; Zhang, J.; Qian, S. A Novel Drug–Drug Coamorphous System without Molecular Interactions: Improve the Physicochemical Properties of Tadalafil and Repaglinide. *RSC Adv.* **2019**, *10* (1), 565–583. https://doi.org/10.1039/C9RA07149K.

(36) Lindenberg, M.; Kopp, S.; Dressman, J. B. Classification of Orally Administered Drugs on the World Health Organization Model List of Essential Medicines According to the Biopharmaceutics Classification System. *Eur J Pharm Biopharm* **2004**, *58* (2), 265–278. https://doi.org/10.1016/j.ejpb.2004.03.001.

(37) Chavda, H.; CN, P.; Anand, I. S. Biopharmaceutics Classification System. *Syst. Rev. Pharm.* **2010**, *1*, 62–69. https://doi.org/10.4103/0975-8453.59514.

(38) Dave, R. A.; Morris, M. E. Novel High/Low Solubility Classification Methods for New Molecular Entities. *Int J Pharm* **2016**, *511* (1), 111–126. https://doi.org/10.1016/j.ijpharm.2016.06.060.

(39) Monteiro, P. F.; Silva-Barcellos, N. M.; Caldeira, T. G.; Reis, A. C. C.; Ribeiro, A. S.; Souza, J. D. Effects of Experimental Conditions on Solubility Measurements for BCS Classification in Order to Improve the Biowaiver Guidelines. *Braz. J. Pharm. Sci.* **2021**, *57*, e181083. https://doi.org/10.1590/s2175-97902020000181083.

(40) GONG, Y.; GRANT, D. J. W.; BRITTAIN, H. G. Principles of Solubility. In *Solvent Systems and Their Selection in Pharmaceutics and Biopharmaceutics*; Augustijns, P., Brewster, M. E., Eds.; Biotechnology: Pharmaceutical Aspects; Springer: New York, NY, 2007; pp 1–27. https://doi.org/10.1007/978-0-387-69154-1_1.

(41) Abbott, S. Solubility Science: Principles and Practice.

(42) Leeson, P. D.; Springthorpe, B. The Influence of Drug-like Concepts on Decision-Making in Medicinal Chemistry. *Nat Rev Drug Discov* **2007**, *6* (11), 881–890. https://doi.org/10.1038/nrd2445.

(43) 1236 SOLUBILITY MEASUREMENTS. **2021**, 13.

(44) Webster, A. C.; Nagler, E. V.; Morton, R. L.; Masson, P. Chronic Kidney Disease. *Lancet* **2017**, *389* (10075), 1238–1252. https://doi.org/10.1016/S0140-6736(16)32064-5.

(45) Levey, A. S.; Coresh, J. Chronic Kidney Disease. *The Lancet* **2012**, *379* (9811), 165–180. https://doi.org/10.1016/S0140-6736(11)60178-5.

(46) Babitt, J. L.; Lin, H. Y. Molecular Mechanisms of Hepcidin Regulation: Implications for the Anemia of CKD. *Am J Kidney Dis* **2010**, *55* (4), 726–741. https://doi.org/10.1053/j.ajkd.2009.12.030.

(47) Babitt, J. L.; Lin, H. Y. Mechanisms of Anemia in CKD. *J Am Soc Nephrol* **2012**, *23* (10), 1631–1634. https://doi.org/10.1681/ASN.2011111078.

(48) Johnson, D. W.; Pollock, C. A.; Macdougall, I. C. Erythropoiesis-Stimulating Agent Hyporesponsiveness. *Nephrology (Carlton)* **2007**, *12* (4), 321–330. https://doi.org/10.1111/j.1440-1797.2007.00810.x.

(49) Becker, K.; Saad, M. A New Approach to the Management of Anemia in CKD Patients: A Review on Roxadustat. *Adv Ther* **2017**, *34* (4), 848–853. https://doi.org/10.1007/s12325-017-0508-9.

(50) Brigandi, R. A.; Johnson, B.; Oei, C.; Westerman, M.; Olbina, G.; de Zoysa, J.; Roger, S. D.; Sahay, M.; Cross, N.; McMahon, L.; Guptha, V.; Smolyarchuk, E. A.; Singh, N.; Russ, S. F.; Kumar, S.; PHI112844 Investigators. A Novel Hypoxia-Inducible Factor-Prolyl Hydroxylase Inhibitor (GSK1278863) for Anemia in CKD: A 28-Day, Phase 2A Randomized Trial. *Am J Kidney Dis* **2016**, *67* (6), 861–871. https://doi.org/10.1053/j.ajkd.2015.11.021.

(51) Provenzano, R.; Besarab, A.; Wright, S.; Dua, S.; Zeig, S.; Nguyen, P.; Poole, L.; Saikali, K. G.; Saha, G.; Hemmerich, S.; Szczech, L.; Yu, K. H. P.; Neff, T. B. Roxadustat (FG-4592) Versus Epoetin Alfa for Anemia in Patients Receiving Maintenance Hemodialysis: A Phase 2, Randomized, 6- to 19-Week, Open-Label, Active-Comparator, Dose-Ranging, Safety and Exploratory Efficacy Study. *Am J Kidney Dis* **2016**, *67* (6), 912–924. https://doi.org/10.1053/j.ajkd.2015.12.020.

(52) Besarab, A.; Chernyavskaya, E.; Motylev, I.; Shutov, E.; Kumbar, L. M.; Gurevich, K.; Chan, D. T. M.; Leong, R.; Poole, L.; Zhong, M.; Saikali, K. G.; Franco, M.; Hemmerich, S.; Yu, K.-H. P.; Neff, T. B. Roxadustat (FG-4592): Correction of Anemia in Incident Dialysis Patients. *J Am Soc Nephrol* **2016**, *27* (4), 1225–1233. https://doi.org/10.1681/ASN.2015030241.

(53) Dhillon, S. Roxadustat: First Global Approval. *Drugs* **2019**, *79* (5), 563–572. https://doi.org/10.1007/s40265-019-01077-1.

(54) Chen, N.; Hao, C.; Liu, B.-C.; Lin, H.; Wang, C.; Xing, C.; Liang, X.; Jiang, G.; Liu, Z.; Li, X.; Zuo, L.; Luo, L.; Wang, J.; Zhao, M.-H.; Liu, Z.; Cai, G.-Y.; Hao, L.; Leong, R.; Wang, C.; Liu, C.; Neff, T.; Szczech, L.; Yu, K.-H. P. Roxadustat Treatment for Anemia in Patients Undergoing Long-Term Dialysis. *N Engl J Med* **2019**, *381* (11), 1011–1022. https://doi.org/10.1056/NEJMoa1901713.

(55) Czock, D.; Keller, F. Clinical Pharmacokinetics and Pharmacodynamics of Roxadustat. *Clin Pharmacokinet* **2022**, *61* (3), 347–362. https://doi.org/10.1007/s40262-021-01095-x.

(56) Akizawa, T.; Iwasaki, M.; Otsuka, T.; Reusch, M.; Misumi, T. Roxadustat Treatment of Chronic Kidney Disease-Associated Anemia in Japanese Patients Not on Dialysis: A Phase 2, Randomized, Double-Blind, Placebo-Controlled Trial. *Adv Ther* **2019**, *36* (6), 1438–1454. https://doi.org/10.1007/s12325-019-00943-4.

(57) Chen, N.; Hao, C.; Peng, X.; Lin, H.; Yin, A.; Hao, L.; Tao, Y.; Liang, X.; Liu, Z.; Xing, C.; Chen, J.; Luo, L.; Zuo, L.; Liao, Y.; Liu, B.-C.; Leong, R.; Wang, C.; Liu, C.; Neff, T.; Szczech, L.; Yu, K.-H. P. Roxadustat for Anemia in Patients with Kidney Disease Not Receiving Dialysis. *NEJM* **2019**, *381* (11), 1001–1010. https://doi.org/10.1056/NEJMoa1813599.

(58) Doogue, M. P.; Polasek, T. M. The ABCD of Clinical Pharmacokinetics. *Ther Adv Drug Saf* **2013**, *4* (1), 5–7. https://doi.org/10.1177/2042098612469335.

(59) Bolleddula, J.; Brady, K.; Bruin, G.; Lee, A. J.; Martin, J. A.; Walles, M.; Xu, K.; Yang, T.-Y.; Zhu, X.; Yu, H. Absorption, Distribution, Metabolism, and Excretion (ADME) of Therapeutic Proteins: Current Industry Practices and Future Perspectives. *Drug Metab Dispos* **2022**. https://doi.org/10.1124/dmd.121.000461.

(60) Vugmeyster, Y.; Harrold, J.; Xu, X. Absorption, Distribution, Metabolism, and Excretion (ADME) Studies of Biotherapeutics for Autoimmune and Inflammatory Conditions. *AAPS J* **2012**, *14* (4), 714–727. https://doi.org/10.1208/s12248-012-9385-y.

(61) Shulpekova, Y.; Nechaev, V.; Kardasheva, S.; Sedova, A.; Kurbatova, A.; Bueverova, E.; Kopylov, A.; Malsagova, K.; Dlamini, J. C.; Ivashkin, V. The Concept of Folic Acid in Health and Disease. *Molecules* **2021**, *26* (12), 3731. https://doi.org/10.3390/molecules26123731.

(62) *Folic Acid - an overview | ScienceDirect Topics*. https://www.sciencedirect.com/topics/pharmacology-toxicology-and-pharmaceutical-science/folic-acid (accessed 2023-08-15).

(63) Mandai, T.; Yoneyama, M.; Sakai, S.; Muto, N.; Yamamoto, I. The Crystal Structure and Physicochemical Properties of L-Ascorbic Acid 2-Glucoside. *Carbohydr Res* **1992**, *232* (2), 197–205. https://doi.org/10.1016/0008-6215(92)80054-5.

(64) Sabbah (France, Chairman), R.; Xu-wu (China), A.; Chickos (Usa), J. S.; Leitão (Portugal), M. L. P.; Roux (Spain), M. V.; Torres (México), L. A. Reference Materials for

Calorimetry and Differential Thermal Analysis. *Thermochimica Acta* **1999**, *331* (2), 93–204. https://doi.org/10.1016/S0040-6031(99)00009-X.

(65) Nangare, S.; Vispute, Y.; Tade, R.; Dugam, S.; Patil, P. Pharmaceutical Applications of Citric Acid. *FJPS* **2021**, *7* (1), 54. https://doi.org/10.1186/s43094-021-00203-9.

(66) Carr, A. C.; Cook, J. Intravenous Vitamin C for Cancer Therapy - Identifying the Current Gaps in Our Knowledge. *Front Physiol* **2018**, *9*, 1182. https://doi.org/10.3389/fphys.2018.01182.

(67) Cysewski, P.; Przybyłek, M.; Ziółkowska, D.; Mroczyńska, K. Exploring the Cocrystallization Potential of Urea and Benzamide. *J Mol Model* **2016**, *22*, 103. https://doi.org/10.1007/s00894-016-2964-6.

(68) Shewale, S.; Shete, A. S.; Doijad, R. C.; Kadam, S. S.; Patil, V. A.; Yadav, A. V. Formulation and Solid State Characterization of Nicotinamide-Based Co-Crystals of Fenofibrate. *Indian J Pharm Sci* **2015**, *77* (3), 328–334.

(69) Li, J.; Bourne, S. A.; Caira, M. R. New Polymorphs of Isonicotinamide and Nicotinamide. *Chem Commun (Camb)* **2011**, *47* (5), 1530–1532. https://doi.org/10.1039/c0cc04117c.

(70) Abourahma, H.; Cocuzza, D. S.; Melendez, J.; Urban, J. M. Pyrazinamide Cocrystals and the Search for Polymorphs. *CrystEngComm* **2011**, *13* (21), 6442–6450. https://doi.org/10.1039/C1CE05598D.

(71) Aitipamula, S.; Chow, P. S.; Tan, R. B. H. Co-Crystals of Caffeine and Piracetam with 4-Hydroxybenzoic Acid: Unravelling the Hidden Hydrates of 1 : 1 Co-Crystals. *CrystEngComm* **2012**, *14* (7), 2381–2385. https://doi.org/10.1039/C2CE25080B.

(72) Bučar, D.-K.; Henry, R. F.; Lou, X.; Duerst, R. W.; MacGillivray, L. R.; Zhang, G. G. Z. Cocrystals of Caffeine and Hydroxybenzoic Acids Composed of Multiple Supramolecular Heterosynthons: Screening via Solution-Mediated Phase Transformation and Structural Characterization. *Cryst. Growth Des.* **2009**, *9* (4), 1932–1943. https://doi.org/10.1021/cg801178m.

(73) Eddleston, M. D.; Hejczyk, K. E.; Bithell, E. G.; Day, G. M.; Jones, W. Determination of the Crystal Structure of a New Polymorph of Theophylline. *Chemistry* **2013**, *19* (24), 7883–7888. https://doi.org/10.1002/chem.201204369.

(74) Trask, A. V.; Motherwell, W. D. S.; Jones, W. Physical Stability Enhancement of Theophylline via Cocrystallization. *Int J Pharm* **2006**, *320* (1–2), 114–123. https://doi.org/10.1016/j.ijpharm.2006.04.018.

(75) Nugrahani, I.; Jessica, M. A. Amino Acids as the Potential Co-Former for Co-Crystal Development: A Review. *Molecules* **2021**, *26* (11), 3279. https://doi.org/10.3390/molecules26113279.

(76) Parra, M.; Stahl, S.; Hellmann, H. Vitamin B6 and Its Role in Cell Metabolism and Physiology. *Cells* **2018**, *7* (7), 84. https://doi.org/10.3390/cells7070084.

(77) Ganduri, R.; Cherukuvada, S.; Guru Row, T. N. Multicomponent Adducts of Pyridoxine: An Evaluation of the Formation of Eutectics and Molecular Salts. *Cryst. Growth Des.* **2015**, *15* (7), 3474–3480. https://doi.org/10.1021/acs.cgd.5b00546.

(78) Goswami, P. K.; Kumar, V.; Ramanan, A. Multicomponent Solids of Diclofenac with Pyridine Based Coformers. *J. Mol. Struct.***2020**, *1210*, 128066. https://doi.org/10.1016/j.molstruc.2020.128066.

(79) Arhangelskis, M.; Lloyd, G. O.; Jones, W. Mechanochemical Synthesis of Pyrazine:Dicarboxylic Acid Cocrystals and a Study of Dissociation by Quantitative Phase Analysis. *CrystEngComm* **2012**, *14* (16), 5203–5208. https://doi.org/10.1039/C2CE25121C.

(80) Friščić, T. Supramolecular Concepts and New Techniques in Mechanochemistry: Cocrystals, Cages, Rotaxanes, Open Metal–Organic Frameworks. *Chem. Soc. Rev.* **2012**, *41* (9), 3493–3510. https://doi.org/10.1039/C2CS15332G.

(81) James, S. L.; Adams, C. J.; Bolm, C.; Braga, D.; Collier, P.; Friščić, T.; Grepioni, F.; Harris, K. D. M.; Hyett, G.; Jones, W.; Krebs, A.; Mack, J.; Maini, L.; Orpen, A. G.; Parkin, I. P.; Shearouse, W. C.; Steed, J. W.; Waddell, D. C. Mechanochemistry: Opportunities for New and Cleaner Synthesis. *Chem. Soc. Rev.* **2011**, *41* (1), 413–447. https://doi.org/10.1039/C1CS15171A.

(82) Hasa, D.; Schneider Rauber, G.; Voinovich, D.; Jones, W. Cocrystal Formation through Mechanochemistry: From Neat and Liquid-Assisted Grinding to Polymer-Assisted Grinding. *Angewandte Chemie International Edition* **2015**, *54* (25), 7371–7375. https://doi.org/10.1002/anie.201501638.

(83) Mojumdar, S. C.; Sain, M.; Prasad, R. C.; Sun, L.; Venart, J. E. S. Selected Thermoanalytical Methods and Their Applications from Medicine to Construction. *J Therm Anal Calorim* **2007**, *90* (3), 653–662. https://doi.org/10.1007/s10973-007-8518-5.

(84) Coleman, N. Modulated Temperature Differential Scanning Calorimetry: A Novel Approach to Pharmaceutical Thermal Analysis. *Int. J. Pharm.* **1996**, *135* (1–2), 13–29. https://doi.org/10.1016/0378-5173(95)04463-9.

(85) Craig, D. Q. M.; Royall, P. G. The Use of Modulated Temperature DSC for the Study of Pharmaceutical Systems: Potential Uses and Limitations. *Pharm Res* **1998**, *15* (8), 1152–1153. https://doi.org/10.1023/A:1011967202972.

(86) Dunmur, R. M., Martin. *Spectroscopic Methods in Organic Chemistry*, 2th Edition.; Hesse, M. M., Herbert; Zeeh,Bernd, Series Ed.; Georg Thieme Verlag KG: Stuttgart, 2008. https://doi.org/10.1055/b-003-108602.

(87) Shah, B.; Kakumanu, V. K.; Bansal, A. K. Analytical Techniques for Quantification of Amorphous/Crystalline Phases in Pharmaceutical Solids. *J Pharm Sci* **2006**, *95* (8), 1641–1665. https://doi.org/10.1002/jps.20644.

(88) Bunaciu, A. A.; Udriștioiu, E. G.; Aboul-Enein, H. Y. X-Ray Diffraction: Instrumentation and Applications. *Crit Rev Anal Chem* **2015**, *45* (4), 289–299. https://doi.org/10.1080/10408347.2014.949616.

(89) Fultz, B.; Howe, J. *Transmission Electron Microscopy and Diffractometry of Materials (Fourth Edition)*; Fultz, B., Howe, J., Eds.; Springer: Berlin, 2013.

(90) Baka, E.; Comer, J. E. A.; Takács-Novák, K. Study of Equilibrium Solubility Measurement by Saturation Shake-Flask Method Using Hydrochlorothiazide as Model Compound. *J. Pharm. Biomed. Anal.* **2008**, *46* (2), 335–341. https://doi.org/10.1016/j.jpba.2007.10.030.

(91) Meloun, M.; Pilařová, L.; Javůrek, M.; Pekárek, T. Multiwavelength UV-Metric and PH-Metric Determination of the Dissociation Constants of the Hypoxia-Inducible Factor Prolyl Hydroxylase Inhibitor Roxadustat. *J. Mol. Liq.* **2018**, *268*, 386–402. https://doi.org/10.1016/j.molliq.2018.07.076.

(92) Silva, E. H. da L. Polimorfos e co-cristais - Ativos clássicos e Ativos Emergentes. In *Polimorfos e co-cristais - Ativos clássicos e Ativos Emergentes*; 2017.